4

Point Positioning by Radio Signals

The indoor point positioning for an agent (such as a mobile device) is mostly determined by RF signal-based approaches. The beacons (e.g., reference points and anchors) are installed in a pre-surveyed location, usually described by a local coordinate system. Based on the distance and angle between the beacons and the agent, the agent's location can be determined. The popular fingerprint matching method, which requires a database of the signal features of the pre-surveyed locations, can also provide a point positioning result. It will be introduced in Chapter 5.

There are different sensors that make use of different wireless communication protocols to provide the ranging and angle measurements, including BLE, UWB, Wi-Fi, and 5G. Table 4.1 shows the available measurements of the popular radio signal sensors for indoor point positioning. Their expected performance in terms of the measurements is given in Table 4.1. The resolution and accuracy of their measurements are different according to their designed signal protocols.

{AU: Edit correct?}

This chapter will not cover the acquisition and the tracking parts of radio signals inside the receiver agent because different receiver algorithms are required for different communication protocols. Instead, this chapter focuses on the state and measurement models and the associated estimation theories and challenges for direct range, differential range, and angle-based indoor

Table 4.1
The Radio Signal Sensors and Their Measurements

	Direct Range			Differential Range	Direct Angle
Sensors	**TOA**	**Two-way TOA (round time trip (RTT))**	**RSS-ranging**	**TDOA**	**AOA**
BLE	Not supported	[1, 2]	[3–5]	Not supported	[6, 7]
UWB	[8–13]	[9, 14–16]	Not preferred	[8, 9, 17–20]	[8, 12, 13, 21, 22]
Wi-Fi	[23, 24]	[25–28]	[25, 27, 29]	[25, 29, 30]	[23, 24]
5G	[31–33]	[31, 34]	Not preferred	[31, 35]	[31, 33, 36]

positioning methods. Table 4.2 provides an overview of the states, measurements, and models for different point positioning methods.

There are three assumptions made for the positioning methods in this chapter:

1. There is an active system from the agent's perspective. The agent requests a positioning solution and then the beacons cooperate to provide radio signals for the agent's receiver to generate either timing or angle measurements between the agent and the beacons.
2. All the beacons' locations are known to the agent. It is not impossible to simultaneously determine the beacons' location at the same. This will require SLAM method to be incorporated in the state. The concept of this advanced method will be introduced in Chapter 9.
3. Both the states and measurements are in a local coordinate system (ENU).

The positioning methods introduced are based on weighted least squares (WLS) for easier comparison between direct ranging, differential ranging, and angle methods. The references of popular closed-form expression models that can use LS methods are included for the readers to perform further study.

{AU: Edits correct?}

The organization of this chapter is as follows. Section 4.1 briefly introduces popular time synchronization methods used in IPIN applications, and

Table 4.2
Comparison of Different Point Positioning Methods Using RF Signals in Terms of Measurement, Model, and State

Methods	**Measurement**	**Model**	**State**
Direct range positioning	d_a^i	$d_a^i = \left\|\mathbf{x}_a - \mathbf{x}^i\right\|$ in (4.16)	$\mathbf{x}_a = \begin{bmatrix} x_{e,a} \\ x_{n,a} \\ x_{u,a} \end{bmatrix}$
Differential range positioning (least squares)	$d_a^{(i,j)} = d_a^i - d_a^j$	$d_a^{(i,j)} = \left\|\mathbf{x}_a - \mathbf{x}^i\right\| - \left\|\mathbf{x}_a - \mathbf{x}^j\right\|$ in (4.36)	$\mathbf{x}_a = \begin{bmatrix} x_{e,a} \\ x_{n,a} \\ x_{u,a} \end{bmatrix}$
Differential range positioning (Fang's algorithm)	$d_a^{(i,j)} = d_a^i - d_a^j$	$\begin{aligned} &-2x_{e,a}\left(x_e^i - x_e^1\right) \\ &-2x_{n,a}\left(x_n^i - x_n^1\right) \\ &= d_a^{i\,2} - d_a^{1\,2} - x_e^{i\,2} \\ &+ x_e^{1\,2} - x_n^{i\,2} + x_n^{1\,2} \end{aligned}$ in (4.45)	$\mathbf{x}_a = \begin{bmatrix} x_{e,a} \\ x_{n,a} \end{bmatrix}$
Differential range positioning (Chan's algorithm)	$c\Delta t^i = d_a^i - d_a^1$	$\begin{aligned} &2\left(x_e^1 - x_e^i\right)x_{e,a} + 2\left(x_n^1 - x_n^i\right)x_{n,a} \\ &-2d_a^1 c\Delta t^i = \left(c\Delta t^i\right)^2 \\ &-\left[\left(x_e^{i\,2} + x_n^{i\,2}\right) - \left(x_e^{1\,2} + x_n^{1\,2}\right)\right] \end{aligned}$ in (4.58)	$\mathbf{x}_a = \begin{bmatrix} x_{e,a} \\ x_{n,a} \\ d_a^1 \end{bmatrix}$
Angle-based positioning (least squares)	$\mathbf{z}_a^i = \begin{bmatrix} \sin\theta_a^i \\ \tan\psi_a^i \end{bmatrix}$	$\begin{aligned} \sin\theta_a^i &= \frac{x_u^i - x_{u,a}}{\left\|\mathbf{x}_a - \mathbf{x}^i\right\|} \\ \tan\psi_a^i &= \frac{x_e^i - x_{e,a}}{x_n^i - x_{n,a}} \end{aligned}$ in (4.63) and (4.64)	$\mathbf{x}_a = \begin{bmatrix} x_{e,a} \\ x_{n,a} \\ x_{u,a} \end{bmatrix}$
Angle-based positioning (OVE)	θ_a^i and ψ_a^i	$\mathbf{S}_a\mathbf{x}_a = \mathbf{z}_a$ in (4.84)	$\mathbf{x}_a = \begin{bmatrix} x_{e,a} \\ x_{n,a} \\ x_{u,a} \end{bmatrix}$
Angle-based positioning (3-D PLE)	θ_a^i and ψ_a^i	$\mathbf{S}_a \begin{bmatrix} x_{e,a} \\ x_{n,a} \end{bmatrix} = \mathbf{z}_a$ in (4.90) $\tan\theta_a^i = \frac{x_u^i - x_{u,a}}{\left\|\mathbf{x}_a(1:2) - \mathbf{x}^i(1:2)\right\|}$ in (4.93)	$\begin{bmatrix} x_{e,a} \\ x_{n,a} \end{bmatrix}$ and $x_{u,a}$

Sections 4.2, 4.3, and 4.4 introduce the measurement model, state model, and the estimation for direct-ranging, differential-ranging, and AOA-based point positioning methods, respectively. Section 4.4 details the common challenges and issues faced by the radio signal-based point positioning methods. Section 4.5 gives coding examples for the three point-positioning methods introduced in the first three sections. The equations mentioned in this chapter will be used to program the positioning algorithms.

4.1 Time Synchronization Methods

High-precision time synchronization is fundamental to accurate point positioning in IPIN applications, where even small timing errors can lead to significant localization inaccuracies. Various synchronization methods are used depending on the required accuracy and system constraints, with performance ranging from subnanosecond to millisecond levels. Table 4.3 provides a comparison of different time synchronization methods.

For the high-end methods, IEEE 1588 Precision Time Protocol (PTP) is a widely used synchronization method that achieves nanosecond-level accuracy in networks supporting UWB TDOA, Wi-Fi RTT, and 5G NR positioning.

Table 4.3
Comparison of Different Time Synchronization Methods Usually Used in IPIN Applications

Synchronization Method	Common Use Cases	Accuracy
IEEE 1588 PTP [37]	UWB, TDOA, Wi-Fi FTM, 5G NR	Nanosecond
White Rabbit (WR) [38]	High-precision indoor systems	Subnanosecond
NTP [39]	Low-precision systems (BLE, Wi-Fi RSSI)	Millisecond
GPSDO [40]	Hybrid outdoor/indoor, UWB TDOA	Microsecond
SyncE [41]	Ethernet-connected anchor networks	Submicrosecond
Proprietary RF Sync [42]	UWB, BLE, Wi-Fi AOA/RTT	Nanosecond-microsecond
5G/LTE Sync [43]	Cellular-based positioning (TDOA, RTT)	Submicrosecond

It works by exchanging timestamped synchronization messages between a master clock and multiple slave clocks in a network, allowing devices to align their time to within nanosecond precision. The protocol uses Sync and Follow-up messages from the master, along with Delay Request and Delay Response messages from the slaves, to compensate for network delays and adjust local clocks accordingly. This allows distributed beacons or anchors to share a synchronized time reference, ensuring that time-based positioning methods can measure precise signal travel times. For example, in UWB-based TDOA, tightly synchronized anchors allow the accurate calculation of a device's position by analyzing differences in signal arrival times, reducing errors to the centimeter scale.

For ultrahigh precision applications, White Rabbit extends IEEE 1588 PTP with subnanosecond synchronization, making it the gold standard for scientific and industrial-grade, high-precision indoor positioning systems. White Rabbit ensures that clock discrepancies remain below a nanosecond, which is essential for laboratory environments, large-scale industrial automation, and sensor fusion applications where ultrafine timing control is required.

GPS Disciplined Oscillators (GPSDOs) are also used in hybrid indoor/outdoor positioning, particularly in UWB TDOA deployments where anchors need a common absolute time reference. GPSDOs ensure microsecond-level synchronization, which is sufficient for most indoor navigation applications where absolute positioning accuracy is required, such as in indoor-outdoor transition areas. However, the GPS receiver is heavily challenged in urban areas, making its accuracy compromised.

Synchronous Ethernet (SyncE) provides submicrosecond accuracy for Ethernet-connected anchor networks, stabilizing clock frequencies across wired infrastructure. SyncE is commonly used alongside IEEE 1588 PTP to eliminate frequency drift in positioning networks, ensuring stable and precise timestamping for Wi-Fi RTT, AOA, and UWB positioning.

At the lower end of the spectrum, Network Time Protocol (NTP) is a software-based synchronization method used in BLE and Wi-Fi RSSI-based positioning systems. However, with millisecond-level accuracy, NTP is unsuitable for high-precision applications. The large timing errors translate to meter-scale position errors, making it impractical for time-sensitive ranging techniques such as TOA or TDOA.

Also, there are proprietary RF synchronization methods. These are commonly found in UWB and BLE AOA-based positioning and offer a flexible alternative in which wired synchronization is infeasible. These systems can achieve nanosecond-to-microsecond accuracy, depending on radio propagation

conditions and hardware capabilities. For example, UWB anchors can use wireless synchronization beacons to align their internal clocks within a few nanoseconds, ensuring robust performance in real-time tracking applications.

Finally, 5G and LTE synchronization provide submicrosecond accuracy for cellular-based positioning (TDOA and RTT methods). By leveraging GPS synchronization and network-wide timing protocols, 5G base stations can align timestamps to nanosecond precision. Again, this is similar to GPSDOs, the GPS-based synchronization will be compromised in urban areas.

4.2 Direct Range-Based Indoor Positioning

As mentioned in the assumption made in this chapter, the location of the beacons is pre-surveyed and is assumed to be known to the agent. If the ranges between the beacons and the agent can be measured by the receiver, the trilateration can be used to determine the agent's location, as shown in Figure 4.1. Taking the beacon's location as the center, the range between the beacon and the agent as the radius, the agent's location is in the circumference. As there could be more than one beacon, the number of the circle is more than 1 as well. If the ranging measurements and the beacons' location are ideal (perfect), the intersection of the circles is a point, indicating the agent's location.

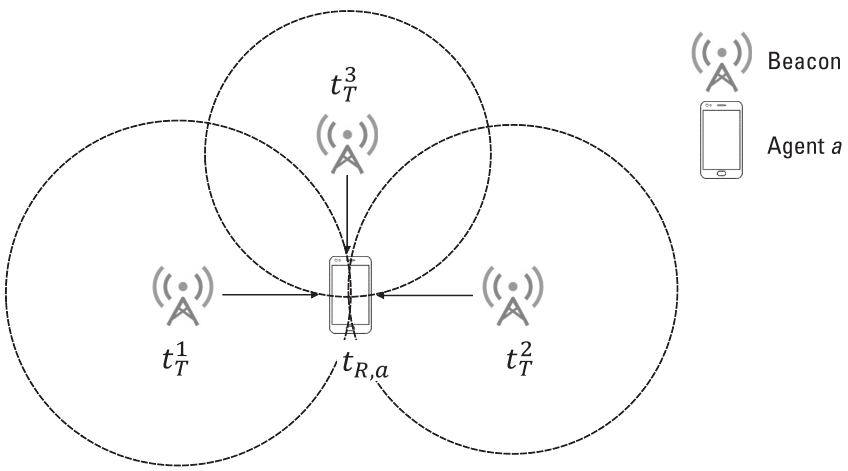

Figure 4.1 The trilateration based on the ranging measurements for indoor point positioning.

4.2.1 Direct Ranging

This section will introduce the three methods, TOA, two-way TOA, and RSS ranging, to generate the direct ranging measurement. More specifically, their models and the use of the measurements to estimate the agent's location will be detailed.

4.2.1.1 TOA Measurement

The direct range measurement based on TOA is generated using:

$$d_a^i = c\left(t_{R,a} - t_T^i\right) \tag{4.1}$$

where the superscript i denotes the index of the beacon, d_a^i denotes the range between beacon i and the target agent a, $t_{R,a}$, and t_T^i denote the time of reception on the agent a and transmission from the beacon i, respectively. Both $t_{R,a}$ and t_T^i are measured by the agent's receiver, and c is the speed of light. This equation holds under two major assumptions: (1) the time is synchronized between the beacons, and (2) the time is synchronized between the beacons and the agent. If we remove both assumptions, then

$$d_a^i = c\left(t_{R,a} - t_T^i + \Delta t_{R,a}^i\right) \tag{4.2}$$

where $\Delta t_{R,a}^i$ is the time-offset between the time of beacon i and the agent a. Obviously, (4.2) always adds one more unknown to the system for each additional beacon, which is not beneficial to the estimation of the agent's location. The first assumption is possible if the indoor beacons are synchronized to an acceptable accuracy by sophisticated synchronization methods, including IEEE 1588 PTP. For the second assumption, it is harder in the TOA measurement-based method because the oscillator used in the agent's receiver is usually low-cost and less stable compared to those used in beacons. Thus, if only the second assumption is removed, then

$$d_a^i = c\left(t_{R,a} - t_T^i + \Delta t_{R,a}\right) \tag{4.3}$$

where the $\Delta t_{R,a}$ is the time offset between the system time of beacons and the agent a, which is an additional unknown to the system. In general, (4.1) or (4.3) is used. However, it is important to consider the noise after applying the corrections of the time offset (usually generated by the beacon system provider and the receiver manufacturer) are used. As a result, the equations become

$$\tilde{d}_a^i = c\left(t_{R,a} - t_T^i\right) + \omega_{\Delta t_{R,a}^i} + \omega_{\Delta t_{R,a}} \tag{4.4}$$

$$\tilde{d}_a^i = c\left(t_{R,a} - t_T^i + \Delta t_{R,a}\right) + \omega_{\Delta t_{R,a}^i} \tag{4.5}$$

where $\omega_{\Delta t_{R,a}^i} \sim \mathcal{N}\left(0, \sigma^2_{\Delta t_{R,a}^i}\right)$ and $\omega_{\Delta t_{R,a}} \sim \mathcal{N}\left(0, \sigma^2_{\Delta t_{R,a}}\right)$ are the Gaussian random noise accounting for the noises after the time correction to synchronize the beacons (which is determined based on different time synchronization methods) and the time correction to synchronize the beacon and the agent, respectively. Note that the estimated time offsets are assumed to be unbiased in this book. If there is 1 ns of error (exemplified by IEEE 1588 PTP) in the time offset correction, then there is about 0.3m of error in the ranging measurement. Thus, it is utterly important to keep the beacons synchronized accurately. It is much harder to obtain the time offset between the agent and the beacons. Thus, the time offset between the system time of beacons and the agent is treated as a state to be estimated when using TOA-based measurement.

4.2.1.2 Two-Way TOA Measurement

The concept of two-way TOA aims to relax the strict time synchronization requirements in two aspects: (1) between beacons, and (2) between the beacon and the agent. In general, NTP, which achieves millisecond-level accuracy, is sufficient for most IPIN applications. This process is illustrated in Figure 4.2, where the signal travels in a round-trip path, making it commonly known

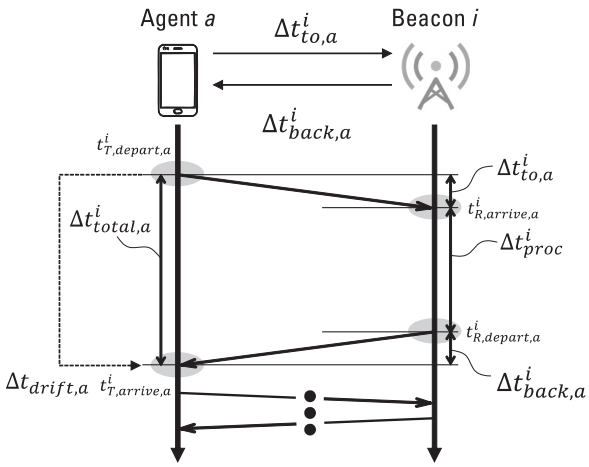

Figure 4.2 The time traveled to generate a two-way TOA ranging measurement.

as the round-trip time (RTT) method. In Wi-Fi Fine Time Measurement (FTM), this approach is explicitly defined as the RTT-based ranging method.

The distance between the agent a and the beacon i can be generated as:

$$d_a^i = c\frac{\left(\Delta t_{\text{to},a}^i + \Delta t_{\text{back},a}^i\right)}{2} \tag{4.6}$$

where $\Delta t_{\text{to},a}^i$ and $\Delta t_{\text{back},a}^i$ denote the time traveled from the agent a to the beacon i and from the beacon back to the agent, respectively. This equation assumes:

1. The beacon processes and retransmits the signal instantaneously (i.e., zero processing time).
2. The agent's clock is perfectly stable (i.e., no clock drift).

In real-world systems, beacons require finite time to process incoming signals before retransmitting them. To account for this processing delay (Δt_{proc}^i), the distance equation is updated to:

$$d_a^i = c\frac{\left(t_{T,\text{arrive},a}^i - t_{T,\text{depart},a}^i\right) - \Delta t_{\text{proc}}^i}{2} \tag{4.7}$$

where $t_{T,\text{depart},a}^i$ and $t_{T,\text{arrive},a}^i$ are the timestamps recorded by the agent when the signal departs and returns, respectively. Δt_{proc}^i is the processing time at the beacon, which must be estimated for accurate distance measurement. The accuracy of Δt_{proc}^i depends on the beacon's oscillator stability. This processing time is typically estimated using timestamps at the beacon upon receiving and transmitting the signal [30, 55]. As processing time estimation significantly affects two-way TOA accuracy, manufacturers often treat it as a proprietary method, using custom calibration strategies to improve performance. Some manufacturers implement adaptive calibration algorithms, while others enforce a fixed processing delay to ensure consistency across beacons. This alternative approach is to define Δt_{proc}^i as a constant, where the beacon deliberately waits for a prespecified duration before retransmitting. This method, although less commonly used in practice, simplifies calibration and ensures consistency in signal processing time [14]. It also provides the beacon with sufficient time to modulate the necessary information into the response signal, which may be beneficial in certain applications.

{AU: References must be called out in sequential order; please call out references 44 to 54 sequentially before reference 55}

The agent's oscillator also introduces timing errors due to clock drift, which accumulates over the total round-trip signal travel time and the beacon's

processing time. If the agent's clock drifts by only 1 ns, it introduces a 0.3-m ranging error. To address this, the model is refined to:

$$d_a^i = c\frac{\left(t_{T,\text{arrive},a}^i - t_{T,\text{depart},a}^i\right) - \Delta t_{\text{proc}}^i - \Delta t_{\text{drift},a}}{2} \tag{4.8}$$

where $\Delta t_{\text{drift},a}$ is the drift-induced error in the agent's clock. In practical systems, temperature-compensated crystal oscillators (TCXOs), Kalman filtering, or external synchronization methods are commonly used to mitigate drift errors.

After accounting for noise introduced by both processing time estimation and clock drift compensation, the final range measurement is modeled as:

$$\tilde{d}_a^i = c\frac{\left(t_{T,\text{arrive},a}^i - t_{T,\text{depart},a}^i\right) - \Delta t_{\text{proc}}^i - \Delta t_{\text{drift},a}}{2} + \omega_{\Delta t_{\text{proc}}^i} + \omega_{\Delta t_{\text{drift},a}} \tag{4.9}$$

where $\omega_{\Delta t_{\text{proc}}^i} \sim \mathcal{N}\left(0,\sigma^2_{\Delta t_{\text{proc}}^i}\right)$ represents Gaussian noise from beacon processing time estimation, and $\omega_{\Delta t_{\text{drift},a}} \sim \mathcal{N}\left(0,\sigma^2_{\Delta t_{\text{drift},a}}\right)$ represents Gaussian noise from clock drift calibration at the agent. The standard deviations $\sigma^2_{\Delta t_{\text{proc}}^i}$ and $\sigma^2_{\Delta t_{\text{drift},a}}$ can typically be obtained from the fact sheets of the beacon and agent receiver hardware [44, 45]. These noise factors highlight the importance of high-quality oscillators and precise calibration in achieving accurate and reliable two-way ranging measurements.

4.2.1.3 RSS Ranging Measurement

Besides relying on the signal propagation time span, the range between a beacon and an agent can also be estimated based on the variation of the radio signal strength (RSS), namely, RSS ranging. Following the path-loss model [46], the strength of a radio signal decays along its propagation path from the beacon (transmitter), as Figure 4.3 demonstrates.

The relationship in between is commonly described by a one-slope model, using

$$p_{R,a}^i = p_{\text{ref}} - 10\eta\log\left(\frac{d_a^i}{d_{\text{ref}}}\right) \tag{4.10}$$

where $P_{R,a}^i$ is the received signal power from the agent a with a distance d_a^i from the beacon i, p_{ref} is the measured power from a reference location with a distance d_{ref} from the beacon, η is the path-loss propagation coefficient

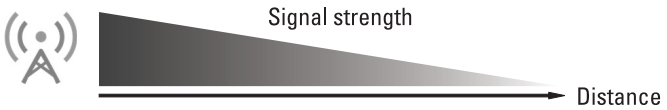

Figure 4.3 The radio signal strength decays along with its propagation distance.

indicating how the RSS decays along with propagation distance. Note that both the agent and the reference location have a certain distance from the beacon fulfilling the far-field assumption to apply the path-loss model. Therefore, it is feasible to inversely estimate the signal propagation distance based on the RSS measurement from the agent [47], as follows.

$$d_a^i = d_{\text{ref}} \cdot 10^{\frac{p_{\text{ref}} - p_{R,a}^i}{10\eta}} \tag{4.11}$$

Unlike the timing-based ranging methods, RSS ranging rely much less on time synchronization or oscillator quality. However, the RSS measurement still contains random variations in space and time [47], which can be modeled as

$$\tilde{p}_{R,a}^i = p_{R,a}^i + \omega_{\text{long},\mathbf{x}_a} + \omega_{\text{short},t} \tag{4.12}$$

where $\omega_{\text{long},\mathbf{x}_a}$ is the space-dependent error term, commonly known as the long-term fading process, $\omega_{\text{short},t}$ is the time-dependent error term, commonly known as the short-term fading process. The short-term fading process can be assumed as stationary and ergodic. Thus, its degradation can be mitigated by the averaging process on multiple samples over certain times, in which the mean value will be absorbed into the reference power term p_{ref} remaining constant [48]. However, the long-term fading process depends on the location of the agent and the surrounding environment, such as the severity of scattering effects. It cannot be mitigated via time averaging but is usually modeled as $\omega_{\text{long},\mathbf{x}_a} \sim \mathcal{N}(0, \sigma^2_{\text{long},\mathbf{x}_a})$ in the scale of dB [47]. Thus, the RSS ranging estimation yields

$$\begin{aligned} \tilde{d}_a^i &= d_{\text{ref}} \cdot 10^{\frac{p_{\text{ref}} - \tilde{p}_{R,a}^i}{10\eta}} = d_{\text{ref}} \cdot 10^{\frac{p_{\text{ref}} - p_{R,a}^i - \omega_{\text{long},\mathbf{x}_a}}{10\eta}} \\ &= d_{\text{ref}} \cdot 10^{\frac{p_{\text{ref}} - p_{R,a}^i}{10\eta}} \cdot 10^{\frac{-\omega_{\text{long},\mathbf{x}_a}}{10\eta}} \end{aligned} \tag{4.13}$$

where the long-term fading process degrades the RSS ranging as a multiplication factor that $\tilde{d}_a^i = d_a^i \cdot 10^{-\omega_{\text{long},\mathbf{x}_a}/10\eta}$.

In terms of the practicality, this method is practical because many of the radio signals do not include the data of time of transmission and the time of arrival (dated February 2025). For example, Wi-Fi can only provide fine-time measurement after the IEEE 802.11mc protocol, meaning that the earlier version of Wi-Fi cannot support FTM measurement methods.

4.2.2 Models and Estimation: Least Squares

In TOA positioning, the agent's location is estimated based on the absolute distances between the agent and multiple beacons. Because the TOA equations are nonlinear, an iterative weighted least squares (I-WLS) method is applied to iteratively refine the position estimate until convergence. This method is widely used in indoor positioning systems because it efficiently handles nonlinear ranging equations while minimizing the impact of measurement noise through a WLS approach.

The measurement vector and state vector are defined as:

$$\mathbf{z}_a = \begin{bmatrix} d_a^1 \\ \vdots \\ d_a^I \end{bmatrix} \tag{4.14}$$

$$\mathbf{x}_a = \begin{bmatrix} x_{e,a} \\ x_{n,a} \\ x_{u,a} \end{bmatrix} \tag{4.15}$$

where $x_{e,a}$, $x_{n,a}$, and $x_{u,a}$ denote the location of agent a on the East-axis, North-axis, and up-axis of the ENU coordinate system, respectively, and there are total I beacons. Note that this estimation algorithm is also applicable to other Cartesian coordinate systems.

Using trilateration, the TOA measurement model is:

$$d_a^i(\mathbf{x}) = \left\| \mathbf{x}_a - \mathbf{x}^i \right\| = \sqrt{\left(x_{e,a} - x_e^i\right)^2 + \left(x_{n,a} - x_n^i\right)^2 + \left(x_{u,a} - x_u^i\right)^2} \tag{4.16}$$

where $\mathbf{x}^i = (x_e^i, x_n^i, x_u^i)$ represents the known position of the ith beacon on the East-axis, North-axis, and up-axis, respectively. By taking the first order of the Taylor series expansion at initial guess $\mathbf{x}_{a(0)}$, the model is linearized:

$$d_a^i(\mathbf{x}_a) \approx d_a^i\left(\mathbf{x}_{a(0)}\right) + \mathbf{h}_{a(0)}^i\left(\mathbf{x}_a - \mathbf{x}_{a(0)}\right) \tag{4.17}$$

where $\mathbf{h}^{i}_{a(0)}$ is the Jacobian matrix, defined as:

$$\mathbf{h}^{i}_{a(0)} = \begin{bmatrix} \dfrac{x_{e,a(0)} - x^{i}_{e}}{d^{i}_{a}\left(\mathbf{x}_{a(0)}\right)} & \dfrac{x_{n,a(0)} - x^{i}_{n}}{d^{i}_{a}\left(\mathbf{x}_{a(0)}\right)} & \dfrac{x_{u,a(0)} - x^{i}_{u}}{d^{i}_{a}\left(\mathbf{x}_{a(0)}\right)} \end{bmatrix} \tag{4.18}$$

Thus, the linearized system for all beacons is:

$$\delta\mathbf{z}_{a} = \underbrace{\begin{bmatrix} \mathbf{h}^{1}_{a(0)} \\ \mathbf{h}^{2}_{a(0)} \\ \vdots \\ \mathbf{h}^{I}_{a(0)} \end{bmatrix}}_{\mathbf{H}_{a(0)}} \delta\mathbf{x}_{a} \tag{4.19}$$

where $\delta\mathbf{z}_{a}$ is the measurement residual vector, $\delta\mathbf{x}_{a}$ is the state correction vector representing the update to the agent's estimated position, and $\mathbf{H}_{a(0)}$is the line-of-sight (LOS) matrix incorporating the $\mathbf{h}^{i}_{a(0)}$ of each beacon.

If at least four beacons are available ($I >= 4$), the system is overdetermined, allowing for an LS solution:

$$\delta\mathbf{x}_{a} = \left(\mathbf{H}_{a(0)}{}^{\mathrm{T}}\mathbf{H}_{a(0)}\right)^{-1}\mathbf{H}_{a(0)}{}^{\mathrm{T}}\delta\mathbf{z}_{a} \tag{4.20}$$

The estimated agent position is iteratively updated as:

$$\mathbf{x}_{a(1)} = \mathbf{x}_{a(0)} + \delta\mathbf{x}_{a} \tag{4.21}$$

The iteration stops when the update falls below a predefined threshold:

$$\left\|\mathbf{x}_{a(k)} - \mathbf{x}_{a(k-1)}\right\| \leq \text{iteration\_threshold} \tag{4.22}$$

where the threshold is selected based on the required localization accuracy.

If the measurement is unbiased and the associated noise standard deviations are available, the WLS estimation can be conducted to achieve a maximum likelihood estimation (MLE).

$$\begin{aligned} \delta\mathbf{x}_{a} &= \left(\mathbf{H}_{a(0)}{}^{\mathrm{T}}\mathbf{W}_{a}\mathbf{H}_{a(0)}\right)^{-1}\mathbf{H}_{a(0)}{}^{\mathrm{T}}\mathbf{W}_{a}\delta\mathbf{z}_{a} \\ \mathbf{W}_{a} &= \begin{bmatrix} \left(\sigma^{2}_{d^{1}_{a}}\right)^{-1} & \cdots & 0 \\ \vdots & \ddots & \vdots \\ 0 & \cdots & \left(\sigma^{2}_{d^{I}_{a}}\right)^{-1} \end{bmatrix} \end{aligned} \tag{4.23}$$

If the beacons and agent clocks are not synchronized, an additional clock bias term must be estimated. In this case, the state vector is expanded to include the unknown clock offset:

$$\mathbf{x}_a = \begin{bmatrix} x_{e,a} \\ x_{n,a} \\ x_{u,a} \\ c\Delta t_{R,a} \end{bmatrix} \tag{4.24}$$

$$d_a^i\left(\mathbf{x}_a\right) = \sqrt{\left(x_{e,a} - x_e^i\right)^2 + \left(x_{n,a} - x_n^i\right)^2 + \left(x_{u,a} - x_u^i\right)^2} + c\Delta t_{R,a} \tag{4.25}$$

By following the same linearization, the linearized LOS model based on an initial guess becomes

$$\mathbf{H}_{a(0)} = \begin{bmatrix} \dfrac{x_{e,a} - x_e^1}{d_a^1\left(\mathbf{x}_{a(0)}\right)} & \dfrac{x_{n,a} - x_n^1}{d_a^1\left(\mathbf{x}_{a(0)}\right)} & \dfrac{x_{u,a} - x_u^1}{d_a^1\left(\mathbf{x}_{a(0)}\right)} & 1 \\ & \vdots & & \vdots \\ \dfrac{x_{e,a} - x_e^I}{d_a^I\left(\mathbf{x}_{a(0)}\right)} & \dfrac{x_{n,a} - x_n^I}{d_a^I\left(\mathbf{x}_{a(0)}\right)} & \dfrac{x_{u,a} - x_u^I}{d_a^I\left(\mathbf{x}_{a(0)}\right)} & 1 \end{bmatrix} \tag{4.26}$$

In this case, the WLS estimation is performed to obtain the optimal position and clock bias estimate.

4.3 Differential Range-Based Indoor Positioning

TOA-based ranging requires precise time synchronization between beacons and the agent, which can be challenging and costly in practical deployments. To avoid this requirement, TDOA techniques are commonly used.

TDOA eliminates the need for absolute time synchronization by measuring relative time differences between signals received at multiple locations. This technique effectively removes common timing offsets, improving robustness against synchronization errors. It can be implemented in three ways, depending on how the time differences are measured:

1. *TDOA across transmitters:* Also known as uplink TDOA, this method is commonly used for snapshot positioning. Multiple beacons (receivers)

measure the time difference of a signal emitted by an agent. This is more popular for large-scale infrastructure-based tracking for the applications such as a real-time location system adapted in indoor logistic scenarios.

2. *TDOA across receivers:* This is also known as downlink TDOA, where a beacon measures the arrival time differences of signals from multiple agents. This approach is popularly used in cellular positioning, such as LTE/5G.

Their comparison is summarized in Table 4.4. The operations of uplink and download TDOAs are different, but the measurements model is actually the same, which is introduced in the following sections.

4.3.1 TDOA Measurement Across Beacons

To compute TDOA measurements, we first establish the direct range equations between the agent a and two beacons i and j:

$$\begin{aligned} d_a^i &= c\left(t_{R,a} - t_T^i + \Delta t_{R,a}\right) \\ d_a^j &= c\left(t_{R,a} - t_T^j + \Delta t_{R,a}\right) \end{aligned} \tag{4.27}$$

Table 4.4
Comparison Between Uplink and Downlink TDOA

Feature	Uplink TDOA	Downlink TDOA
Who transmits?	Agent (mobile device, tag, tracker)	Fixed beacon (Wi-Fi AP, base station for cell communication)
Who receives?	Fixed infrastructure (multiple beacons)	Mobile agents (phones, vehicles)
Who computes position?	Centralized server or infrastructure	The agent (self-localization)
Scalability	Limited (too many transmitting agents can cause congestion)	Higher (many devices can passively receive signals)
Best for:	Large-scale tracking, RTLS, UWB-based indoor positioning	GNSS-like positioning, LTE/5G-based localization, multi-agent systems
Common applications	Industrial RTLS, logistics, emergency responder tracking	LTE/5G OTDOA, Wi-Fi FTM, autonomous navigation

where

- d_a^i and d_a^j are the distances between the agent and beacons i and j, respectively.
- $\Delta t_{R,a}$ is the receive timestamp at the agent.
- t_T^i and t_T^j are the transmit timestamps at beacons i and j.
- $t_{R,a}$ represents the receiver's clock offset.

By differencing the two direct range equations, we eliminate the receiver's clock offset:

$$d_a^{(i,j)} = d_a^i - d_a^j = c\left(t_{R,a} - t_T^i + \Delta t_{R,a}\right) - c\left(t_{R,a} - t_T^j + \Delta t_{R,a}\right) = c\left(t_T^j - t_T^i\right) \tag{4.28}$$

$d_a^{(i,j)}$ denotes the range difference between the direct ranges of d_a^i and d_a^j. This is a widely used method because receiver clock stability has less impact on range measurements compared to TOA-based methods. Equation (3.27) assumes that beacons are perfectly synchronized. However, in real-world implementations, beacons often operate on independent clocks, introducing an additional time offset $\Delta t_{R,a}^{(i,j)}$ between them. This modifies the equation:

{AU: Do you mean (4.27)?}

$$\begin{aligned} d_a^i &= c\left(t_{R,a} - t_T^i + \Delta t_{R,a}^i\right) \\ d_a^j &= c\left(t_{R,a} - t_T^j + \Delta t_{R,a}^j\right) \\ d_a^{(i,j)} = d_a^i - d_a^j &= c\left(t_{R,a} - t_T^i + \Delta t_{R,a}^i\right) - c\left(t_{R,a} - t_T^j + \Delta t_{R,a}^j\right) \\ &= c\left(t_T^j - t_T^i + \Delta t_{R,a}^{(i,j)}\right) \end{aligned} \tag{4.29}$$

where $\Delta t_{R,a}^{(i,j)}$ represents the unknown time offset between beacons i and j. This introduces an additional unknown in the system, making direct estimation of the agent's position more difficult. Thus, beacon synchronization is generally required for TDOA-based positioning systems, similar to TOA methods [59]. To account for remaining synchronization errors after time correction, Gaussian noise is introduced into the equation:

{AU: Please call out references 49 to 58 sequentially in text}

$$\tilde{d}_a^{i,j} = c\left(t_T^j - t_T^i\right) + \omega_{\Delta t_{R,a}} \tag{4.30}$$

where $\omega_{\Delta t_{R,a}} \sim \mathcal{N}\left(0, \sigma^2_{\Delta t_{R,a}}\right)$ represents random synchronization errors in the beacon clocks.

If beacon synchronization is impractical, an alternative approach is to derive TDOA from two-way TOA measurements. Assuming that the beacons process signals with identical delays (i.e., $t^i_{\text{proc}} = \Delta t^j_{\text{proc}} = \Delta t_{\text{proc}}$), the direct ranges become:

$$\begin{aligned} d^i_a &= c\frac{\left(t^i_{T,\text{arrive},a} - t^i_{T,\text{depart},a}\right) - \Delta t_{\text{proc}}}{2} \\ d^j_a &= c\frac{\left(t^j_{T,\text{arrive},a} - t^j_{T,\text{depart},a}\right) - \Delta t_{\text{proc}}}{2} \end{aligned} \tag{4.31}$$

By differencing the two equations, we obtain:

$$d^{(i,j)}_a = d^i_a - d^j_a = c\frac{\left(t^i_{T,\text{arrive},a} - t^i_{T,\text{depart},a}\right) - \left(t^j_{T,\text{arrive},a} - t^j_{T,\text{depart},a}\right)}{2} \tag{4.32}$$

This equation benefits from:

1. *TDOA:* Eliminates receiver clock offsets.
2. *Two-way TOA:* Avoids requiring beacon synchronization.

As each TDOA measurement requires a pair of beacons, a system with I beacons provides only $I-1$ independent TDOA measurements. Therefore, one beacon (e.g., beacon j) is selected as the reference, and all TDOA measurements are computed relative to it:

$$d^{(i,j)}_a = d^i_a - d^j_a, \ \ \forall i \neq j \tag{4.33}$$

The choice of reference beacon affects the system's geometry and localization accuracy. Typically, the reference beacon is:

- Placed centrally within the deployment area.
- Selected dynamically based on signal strength.

A poor choice of reference beacon can lead to a poor geometric dilution of precision (GDOP), reducing positioning accuracy, which is discussed later in the chapter.

4.3.2 Model and Estimation

TDOA positioning is widely used in wireless localization, radar, and sensor networks. It estimates an unknown signal source's position based on the time

differences between signals arriving at multiple receivers. Various algorithms have been developed to solve this hyperbolic localization problem, with LS estimation, Fang's algorithm, and Chan's algorithm being the most commonly applied. Each method offers a trade-off between computational complexity, accuracy, and robustness.

LS formulates the TDOA problem as a set of nonlinear equations that require iterative optimization. The LS approach is effective in minimizing residual errors but demands an initial position estimate and can be sensitive to poor initialization and convergence issues. When properly initialized, LS

{AU: Call out table sequentially in text}

Table 4.5
Comparison of the Models and Estimation Algorithms Used for TDOA-Based Positioning

Feature	LS Estimation [49]	Fang's Algorithm [50]	Chan's Algorithm [51]
Type of solution	Iterative	Closed-form	Two-step closed-form
Computational complexity	High (iterative updates)	Moderate (single LS step)	Low (sequential LS + quadratic constraint)
Handling of nonlinearity	Requires iterative linearization	Linearized via algebraic manipulation	Uses an auxiliary variable to linearize equations
Robustness to noise	Moderate (relies on noise model)	Sensitive (linearization amplifies errors)	High (WLS refines estimation)
Accuracy	High (converges to machine learning solution if noise is Gaussian)	Moderate (noise-dependent)	High (approaches Cramér-Rao bound for small errors)
Initial guess required?	Yes (iterative convergence)	No (direct LS solution)	No (direct LS + refinement)
Sensitivity to geometric configuration	High (bad initial guess affects convergence)	High (ill-conditioned geometry increases errors)	Lower (redundant measurements reduce GDOP effects)
WLS support	Yes	No	Yes (second step applies WLS)
Solution stability	Can diverge if poorly initialized	Can be unstable for poor anchor placement	More stable due to quadratic constraint correction
Application scenarios	High-precision GNSS, radar tracking	Real-time positioning with minimal computation	Robust localization in wireless networks, UWB, and sensor networks

estimation provides high accuracy and can handle complex error models through iterative refinements.

Fang's algorithm introduces a closed-form approach, transforming the hyperbolic TDOA equations into a linear system using algebraic manipulation. This method eliminates the need for iterative computation, making it computationally efficient. However, its accuracy can degrade in the presence of high measurement noise, and its performance is dependent on a favorable receiver geometry.

Chan's algorithm combines the advantages of LS and Fang's methods by employing a two-step process: first, an initial estimate is obtained through an unweighted LS solution, followed by a WLS refinement that accounts for measurement noise correlation. This approach improves robustness and accuracy, making it well-suited for real-world implementations in UWB, cellular positioning, and GNSS-like localization.

The following sections will provide a detailed mathematical representation of each method, highlighting their formulation for TDOA-based positioning systems.

4.3.3 Least Squares

TDOA positioning relies on solving a set of nonlinear hyperbolic equations, where the agent's position is estimated based on the range differences between pairs of beacons. To solve this problem, we apply the I-WLS method, which iteratively refines the position estimate by linearizing the nonlinear equations and minimizing the squared residuals.

This method is widely used in indoor positioning because it efficiently handles the nonlinear nature of TDOA measurements while providing accurate and computationally efficient solutions.

In this book, an iterative LS estimation is selected as the main point positioning estimation to introduce due to its popularity. Considering (4.27) and (4.30), the measurement vector $\mathbf{z}_a$ and the state vector $\mathbf{x}_a$ are given here:

$$\mathbf{z}_a = \begin{bmatrix} d_a^{1,j} \\ \vdots \\ d_a^{I-1,j} \end{bmatrix} \tag{4.34}$$

$$\mathbf{x}_a = \begin{bmatrix} x_{e,a} \\ x_{n,a} \\ x_{u,a} \end{bmatrix} \tag{4.35}$$

where $x_{e,a}$, $x_{n,a}$, and $x_{u,a}$ denote the agent's location on the East-axis, North-axis, and up-axis of the ENU coordinate system, respectively, and there are $I-1$ beacons with beacon j as the reference beacon.

Using trilateration, the measurement model is:

$$d_a^{(i,j)} = \left\|\mathbf{x}_a - \mathbf{x}^i\right\| - \left\|\mathbf{x}_a - \mathbf{x}^j\right\| \tag{4.36}$$

where $\mathbf{x}^i$ represents the position of the ith beacon at (x_e^i, x_n^i, x_u^i). As shown in the equation above, each TDOA measurement corresponds to a hyperbola equation in 2-D (or a hyperboloid in 3-D). Figure 4.4 illustrates the TDOA model, where beacon 1 serves as the reference beacon. The solid lines are the hyperbola equations that represented the TDOA model of $d_a^{2,1}$ and $d_a^{3,1}$.

Since (4.36) is nonlinear, we apply a first-order Taylor series expansion around an initial position estimate $\mathbf{x}_{a(0)}$ to linearize the model:

$$d_a^{(i,j)}\left(\mathbf{x}_a\right) \approx d_a^{(i,j)}\left(\mathbf{x}_{a(0)}\right) + \mathbf{h}_{a(0)}^{(i,j)}\left(\mathbf{x}_a - \mathbf{x}_{a(0)}\right) \tag{4.37}$$

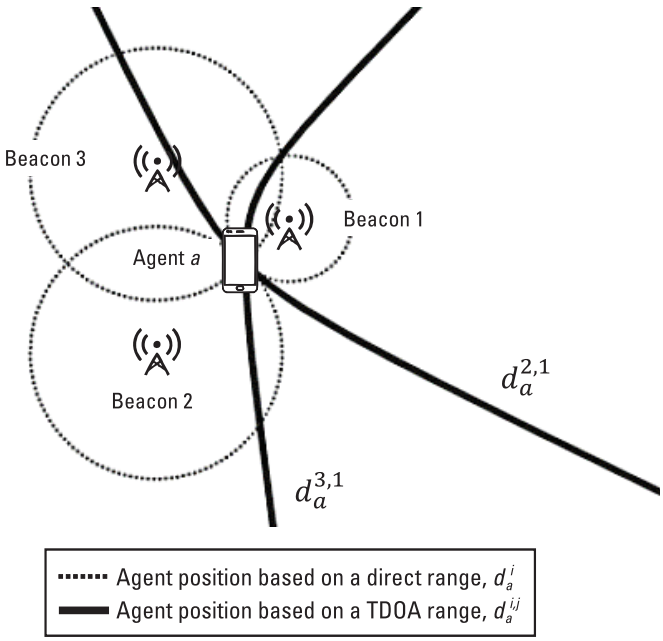

Figure 4.4 The measurement model of TDOA across the beacons. Beacon 1 acts as the reference beacon.

where $\mathbf{h}_{a(0)}^{(i,j)}$ is the Jacobian matrix, defined as:

$$\mathbf{h}_{a(0)}^{(i,j)} == \begin{bmatrix} \dfrac{x_{e,a(0)} - x_e^i}{d_a^i\left(\mathbf{x}_{a(0)}\right)} & \dfrac{x_{n,a(0)} - x_n^i}{d_a^i\left(\mathbf{x}_{a(0)}\right)} & \dfrac{x_{u,a(0)} - x_u^i}{d_a^i\left(\mathbf{x}_{a(0)}\right)} \end{bmatrix} - \begin{bmatrix} \dfrac{x_{e,a(0)} - x_e^j}{d_a^j\left(\mathbf{x}_{a(0)}\right)} & \dfrac{x_{n,a(0)} - x_n^j}{d_a^j\left(\mathbf{x}_{a(0)}\right)} & \dfrac{x_{u,a(0)} - x_u^j}{d_a^j\left(\mathbf{x}_{a(0)}\right)} \end{bmatrix} \tag{4.38}$$

Thus, the linearized system takes the form:

$$\delta\mathbf{z}_a = \mathbf{H}_{a(0)}\delta\mathbf{x}_a \tag{4.39}$$

where $\delta\mathbf{z}_a$ is the measurement residual vector, $\delta\mathbf{x}_a$ is the state correction vector representing the update to the agent's estimated position, and $\mathbf{H}_{a(0)}$ is differenced LOS matrix.

If at least four beacons are available, the system is overdetermined ($I - 1 > 3$) allowing for an LS solution:

$$\delta\mathbf{x}_a = \left(\mathbf{H}_{a(0)}{}^{\mathrm{T}}\mathbf{H}_{a(0)}\right)^{-1}\mathbf{H}_{a(0)}{}^{\mathrm{T}}\delta\mathbf{z}_a \tag{4.40}$$

If the noise statistics of the TDOA measurements are available, a WLS method can be used to an optimal solution.

$$\delta\mathbf{x}_a = \left(\mathbf{H}_{a(0)}{}^{\mathrm{T}}\mathbf{W}_a\mathbf{H}_{a(0)}\right)^{-1}\mathbf{H}_{a(0)}{}^{\mathrm{T}}\mathbf{W}_a\delta\mathbf{z}_a \tag{4.41}$$

where $\mathbf{W}_a$ is the weighting matrix, typically defined as $\mathbf{W}_a = \boldsymbol{\Sigma}_a^{-1}$, where $\boldsymbol{\Sigma}_a$ is the covariance matrix of measurement errors.

$$\boldsymbol{\Sigma}_a = \begin{bmatrix} \sigma^2_{d_a^{1,j}} & \sigma^2_{\text{inter}} & \cdots & \sigma^2_{\text{inter}} \\ \sigma^2_{\text{inter}} & \sigma^2_{d_a^{2,j}} & \cdots & \sigma^2_{\text{inter}} \\ \vdots & \vdots & \ddots & \vdots \\ \sigma^2_{\text{inter}} & \sigma^2_{\text{inter}} & \cdots & \sigma^2_{d_a^{I-1,j}} \end{bmatrix} \tag{4.42}$$

It is important to note that the differenced measurements, meaning the measurements are actually correlated with each other. As a result, the

off-diagonal terms are no longer zeros, denoted as the correction σ^2_{inter} between each TDOA measurement.

4.3.4 Fang's Algorithms

Fang's algorithm is a closed-form LS-based method used for TDOA positioning. It provides a direct algebraic solution to the nonlinear TOA equations by reformulating them into a linear system. Unlike iterative approaches such as nonlinear LS, Fang's method avoids convergence issues and provides a computationally efficient localization solution.

Consider a mobile device at an unknown 2-D position $\mathbf{x}_a = \begin{bmatrix} x_{e,a} \\ x_{n,a} \end{bmatrix}$ with I known reference anchors located at (x_e^i, x_n^i) for $i = 1, 2, \cdots, I$. The TOA measurements provide the estimated distance to each anchor, using

$$d_a^i = \sqrt{\left(x_{e,a} - x_e^i\right)^2 + \left(x_{n,a} - x_n^i\right)^2} + \omega_i \tag{4.43}$$

where d_a^i is the estimated range from the mobile device a to anchor i, and ω_i is the measurement noise.

To derive a closed-form solution, Fang's algorithm linearizes these nonlinear range equations. Choose one of the anchors (e.g., the first anchor) as a reference and define the squared range difference between each anchor i and the reference anchor 1, by

$$\begin{aligned} d_a^{i\,2} - d_a^{1\,2} &= \left(x_{e,a} - x_e^i\right)^2 + \left(x_{n,a} - x_n^i\right)^2 - \left(x_{e,a} - x_e^1\right)^2 - \left(x_{n,a} - x_n^1\right)^2 \\ &= x_{e,a}^2 - 2x_{e,a}x_e^i + x_e^{i\,2} + x_{n,a}{}^2 - 2x_{n,a}x_n^i + x_n^{i\,2} \\ &\quad -x_{e,a}^2 + 2x_{e,a}x_e^1 - x_e^{1\,2} - x_{n,a}^2 + 2x_{n,a}x_n^1 - x_n^{1\,2} \end{aligned} \tag{4.44}$$

The equation can be rearranged as

$$\begin{aligned} &d_a^{i\,2} - d_a^{1\,2} - x_e^{i\,2} + x_e^{1\,2} - x_n^{i\,2} + x_n^{1\,2} \\ &\qquad = -2x_{e,a}\left(x_e^i - x_e^1\right) - -2x_{n,a}\left(x_n^i - x_n^1\right) \end{aligned} \tag{4.45}$$

Regarding the linear system corresponding to $\mathbf{x}_a$, the equation can be rewritten as

{AU: Edits correct?}

$$h_{e,a}^i x_{e,a} + h_{n,a}^i x_{n,a} = y_a^i \tag{4.46}$$

where

$$\begin{aligned} h_{e,a}^{i} &= -2\left(x_e^i - x_e^1\right) \\ h_{n,a}^{i} &= -2\left(x_n^i - x_n^1\right) \\ y_a^i &= d_a^{i\,2} - d_a^{1\,2} - x_e^{i\,2} + x_e^{1\,2} - x_n^{i\,2} + x_n^{1\,2} \end{aligned} \tag{4.47}$$

By incorporating all the anchors, the linear system of the agent's position can be written into a matrix form, by

$$\underbrace{\begin{bmatrix} h_{e,a}^{2} & h_{n,a}^{2} \\ h_{e,a}^{3} & h_{n,a}^{i} \\ \vdots & \vdots \\ h_{e,a}^{I} & h_{n,a}^{I} \end{bmatrix}}_{\mathbf{H}_a} \begin{bmatrix} x_{e,a} \\ x_{n,a} \end{bmatrix} = \underbrace{\begin{bmatrix} y_a^2 \\ y_a^3 \\ \vdots \\ y_a^I \end{bmatrix}}_{\mathbf{y}_a} \tag{4.48}$$

This system can be solved using the LS estimation, as

$$\mathbf{x}_a = \left(\mathbf{H}_a^{\mathrm{T}}\mathbf{H}_a\right)^{-1}\mathbf{H}_a^{\mathrm{T}}\mathbf{y}_a \tag{4.49}$$

where $\mathbf{H}_a$ and $\mathbf{y}_a$ are the matrix and vector incorporating the terms from each anchor from index 2 to I by (4.48). The mobile device's location can be directly obtained by from the LS solution.

As can be seen, Fang's algorithm provides an efficient closed-form solution for TOA-based positioning by transforming nonlinear range equations into a linear system and solving using LS. This approach eliminates the need for iterative methods, making it computationally efficient and numerically stable. Unlike LS algorithms, Fang's method avoids convergence issues and is well-suited for real-time positioning applications in Wi-Fi FTM, UWB, and cellular TOA-based localization. However, Fang's algorithm has limitations. It is sensitive to measurement noise, particularly in multipath environments where TOA estimates may be biased. Additionally, at least three anchors are required for a valid 2-D solution, and poor anchor geometry can lead to GDOP, amplifying positioning errors. Although the LS solution is computationally fast, it does not inherently incorporate error modeling or filtering, making it less robust to noisy or biased TOA measurements compared to statistical estimation techniques such as Kalman filters. Overall, Fang's algorithm strikes a balance between computational simplicity and accuracy, making it

a practical choice when computational efficiency is a priority. However, in high-noise environments, further refinement or hybrid approaches may be needed to enhance robustness.

4.3.5 Chan's Algorithms

Chan's algorithm is a well-known closed-form solution for source localization using TDOA measurements. It provides a noniterative method (via an auxiliary variable approach) to solve the hyperbolic location problem and is valued for its accuracy and efficiency [51]. Unlike earlier hyperbolic positioning methods (e.g., Fang's algorithm), Chan's method can incorporate redundant measurements from extra base stations, improving accuracy by using a two-step WLS approach.

For simplicity, we consider a 2-D plane with an unknown source (or mobile agent) located at $(x_{e,a}, x_{n,a})$. There are I known base stations (anchors) at fixed positions (x_e^i, x_n^i) for $i = 1, 2, \cdots, I$. One of these (e.g., the first anchor) is designated as the reference station. The goal of TDOA-based positioning is to estimate the unknown position of the agent using measured TDOAs between the reference station and the other stations.

The distance between the agent and each station i has the same form as (4.43), in which the noise is assumed to be negligible during estimation. In particular, the reference range for station 1 can be written as

$$d_a^1 = \sqrt{\left(x_{e,a} - x_e^1\right)^2 + \left(x_{n,a} - x_n^1\right)^2} \tag{4.50}$$

where the unknown terms can be used to form the state vector for estimation, as

$$\mathbf{x}_a = \begin{bmatrix} x_{e,a} \\ x_{n,a} \\ d_a^1 \end{bmatrix} \tag{4.51}$$

Here, the distance to the reference station, d_a^1, will be treated as an additional variable to be estimated during positioning.

The TDOA measurement between station i and the reference station (indexed by 1 here):

$$\Delta t^i = t^i - t^1 \tag{4.52}$$

where t^i is the signal arrival time at station i, and t^1 is the arrival time at the reference station. Δt^i is the observed difference in travel time from the source

to station i and to station 1. It relates to the difference in distances by the signal propagation speed (e.g., the speed of radio, c), as follows:

$$c\Delta t^i = d_a^i - d_a^1 \tag{4.53}$$

Thus, the distance from the source to each station i can be written as

$$d_a^i = d_a^1 + c\Delta t^i \tag{4.54}$$

Geometrically, this equation represents a hyperbola: the locus of points for which the range difference, $d_a^i - d_a^1$, is constant. Each pair (i, 1) defines a hyperbolic curve on which the source must lie. With multiple stations, the source is at the intersection of multiple hyperbolae (similar to Figure 4.4).

The range difference equation (4.54) can be expanded in an explicit form as

$$\sqrt{\left(x_{e,a} - x_e^i\right)^2 + \left(x_{n,a} - x_n^i\right)^2} = \sqrt{\left(x_{e,a} - x_e^1\right)^2 + \left(x_{n,a} - x_n^1\right)^2} + c\Delta t^i \tag{4.55}$$

Squaring both sides and rearranging the equation yield

$$\begin{aligned}&\left(x_{e,a} - x_e^i\right)^2 + \left(x_{n,a} - x_n^i\right)^2 - \left(x_{e,a} - x_e^1\right)^2 - \left(x_{n,a} - x_n^1\right)^2 \\ &= 2c\Delta t^i \sqrt{\left(x_{e,a} - x_e^1\right)^2 + \left(x_{n,a} - x_n^1\right)^2} + \left(c\Delta t^i\right)^2\end{aligned} \tag{4.56}$$

By substituting the square root term by (4.50), this becomes

$$\begin{aligned}&\left(x_{e,a} - x_e^i\right)^2 - \left(x_{e,a} - x_e^1\right)^2 + \left(x_{n,a} - x_n^i\right)^2 - \left(x_{n,a} - x_n^1\right)^2 \\ &= 2d_a^1 c\Delta t^i + \left(c\Delta t^i\right)^2\end{aligned} \tag{4.57}$$

- Step 1: Solve a Linearized LS Problem

In this step, we assume that d_a^1 is an unknown constant and solve for the source position using a linearized LS approach. This step ignores the measurement error correlation (treating it as an LS problem) and, in the minimal case, provides a closed-form solution.

We rewrite the TDOA measurement equations in a linear form, introducing d_a^1 as an auxiliary unknown, as follows

$$\begin{aligned}&2\left(x_e^1 - x_e^i\right)x_{e,a} + 2\left(x_n^1 - x_n^i\right)x_{n,a} - 2d_a^1 c\Delta t^i \\ &= \left(c\Delta t^i\right)^2 - \left[\left(x_e^{i\,2} + x_n^{i\,2}\right) - \left(x_e^{1\,2} + x_n^{1\,2}\right)\right]\end{aligned} \tag{4.58}$$

Incorporating the TDOA measurement equations of all the stations (index from 2 to I), the system equation can be written in a matrix form, as

$$\underbrace{\begin{bmatrix} h_{e,a}^2 & h_{n,a}^2 & 2c\Delta t^2 \\ h_{e,a}^3 & h_{n,a}^3 & 2c\Delta t^3 \\ \vdots & \vdots & \vdots \\ h_{e,a}^I & h_{n,a}^I & 2c\Delta t^I \end{bmatrix}}_{\mathbf{H}_a} \begin{bmatrix} x_{e,a} \\ x_{n,a} \\ d_a^1 \end{bmatrix} = \underbrace{\begin{bmatrix} y_a^2 \\ y_a^3 \\ \vdots \\ y_a^I \end{bmatrix}}_{\mathbf{y}_a} \tag{4.59}$$

where

$$\begin{aligned} h_{e,a}^i &= 2\left(x_e^1 - x_e^i\right) \\ h_{n,a}^i &= 2\left(x_n^1 - x_n^i\right) \\ y_a^i &= \left(c\Delta t^i\right)^2 - \left[\left(x_e^{i\,2} + x_n^{i\,2}\right) - \left(x_e^{1\,2} + x_n^{1\,2}\right)\right] \end{aligned} \tag{4.60}$$

This forms the basis for Chan's estimation approach. If $I \geq 4$, the system is overdetermined, and the LS estimate is obtained by the same approach as (4.49). This provides an initial estimate of the state $\mathbf{x}_a$ for the source position.

- Step 2: WLS Refinement

The first step does not account for the error covariance of TDOA measurements, which are correlated due to the common reference station. The second step refines the estimate using a WLS solution, which incorporates the covariance matrix $\boldsymbol{\Sigma}$ of measurement errors. The WLS estimate is given by

$$\mathbf{x}_a = \left(\mathbf{H}_a^{\mathrm{T}} \boldsymbol{\Sigma}^{-1} \mathbf{H}_a\right)^{-1} \mathbf{H}_a^{\mathrm{T}} \boldsymbol{\Sigma}^{-1} \mathbf{y}_a \tag{4.61}$$

where $\boldsymbol{\Sigma}$ is the error covariance matrix, given by

$$\boldsymbol{\Sigma}_a = \begin{bmatrix} \sigma_{2,1}^2 & \sigma_1^2 & \cdots & \sigma_1^2 \\ \sigma_1^2 & \sigma_{3,1}^2 & \cdots & \sigma_1^2 \\ \vdots & \vdots & \ddots & \vdots \\ \sigma_1^2 & \sigma_1^2 & \cdots & \sigma_{I,1}^2 \end{bmatrix} \tag{4.62}$$

where $\sigma_{i,1}^2 = \sigma_i^2 + \sigma_1^2$ represents the variance of each range difference measurement and σ_1^2 represents the error contribution from the reference station. By applying the WLS estimate, the final position estimate is obtained, which is more statistically efficient and approaches the maximum likelihood solution for Gaussian noise.

It is worth noting that the quadratic constraint enforcement can yield two symmetric intersection solutions in some cases (geometrically, two possible mirror positions relative to the anchor configuration). Additional information or constraints (such as an initial guess, known bounds, or a third measurement in the 2-D case) can help to identify the correct one. In Chan's original formulation with the minimum three base stations, the ambiguity is resolved by selecting the positive root for d_a^1 (distance must be positive, and typically the smaller root corresponds to the feasible solution within the deployment area) [52]. When more than three stations are used, the LS step tends to bias the solution toward the correct position given all the measurements, and the quadratic correction step then fine-tunes the range consistency.

Chan's algorithm, originally developed for one-way TOA measurements, can be effectively applied to two-way TOA-based localization, such as RTT and Wi-Fi FTM. In these methods, the mobile agent measures the RTT between itself and multiple anchors, deriving the one-way TOA by dividing by two. Mathematically, two-way TOA still provides range estimates to known anchors, preserving the core structure of the TOA equations used in Chan's algorithm. The algorithm's key steps—linearizing the range equations, applying LS estimation, and refining the solution using WLS—remain unchanged. This makes it a practical, closed-form approach that avoids the convergence issues of nonlinear LS methods. Chan's algorithm is a robust choice for two-way TOA positioning, offering a balance between computational efficiency and accuracy. When combined with noise mitigation techniques or filtering methods, it can serve as a reliable foundation for RTT-based indoor localization in Wi-Fi, UWB, and other RF systems.

4.4 Angle-Based Indoor Positioning

Comparing with TOA and TDOA, the angle-based methods are much less relying on the time synchronization between the beacons and the agent. The required accuracy of time synchronization is similar to the required output rate of the positioning solutions. In addition, the angle measurement can directly be used to determine the location of the agent. The angle-based measurement focused is the AOA from the beacons to the agent while the equations derived below can also be applied to the methods for the AOD.

AOA-based positioning methods leverage bearing measurements to estimate an agent's location. Among the various techniques used, LS estimation (LSE), the orthogonal vector estimator (OVE), and the pseudolinear estimator (PLE) are three prominent approaches, each with distinct mathematical formulations, computational requirements, and performance characteristics.

LSE is an iterative method that refines an initial position estimate by minimizing the squared residuals between measured and expected AOA values [53]. It provides the highest accuracy when measurement noise is Gaussian and can incorporate WLS for improved estimation when noise variances are known. However, LSE requires an initial guess and has higher computational complexity due to its iterative nature. It is particularly suitable for high-precision localization applications where accuracy is prioritized over computation speed.

OVE introduces a vector-based formulation, solving for the position in a closed-form manner without requiring iterations [54]. By minimizing errors perpendicular to bearing lines, it offers higher accuracy than PLE while maintaining reasonable computational efficiency. However, it remains sensitive to poor geometric configurations and noise. OVE is well-suited for applications that require a balance between computational efficiency and accuracy, such as sensor fusion and autonomous navigation.

PLE, in contrast, is a linearized LS estimator that approximates the AOA equations for direct computation [55]. It is computationally the fastest among the three methods, making it ideal for real-time positioning and low-power embedded systems. However, PLE introduces bias, especially under high noise conditions or poor sensor geometries. It is often used for initial position estimation or scenarios where computational efficiency is critical.

The following sections provide the detailed mathematical formulations of these methods, starting from LSE, followed by the OVE, and concluding with the PLE.

4.4.1 Model and Estimation: IWLS Estimation

In a 3-D positioning scenario, an AOA measurement provides two angular components, the elevation angle θ_{a}^{i}, which measures the vertical angle (i.e., inclination) between the LOS vector (to the agent) and the horizontal plane (North-East plane), and the azimuth angle ψ_{a}^{i}, which measures the horizontal bearing relative to a reference direction (e.g., North in the later explanations), as shown in Figure 4.5.

The AOA measurement models establish a trigonometric relationship between the agent's position and the beacon's position. These can be expressed as:

$$\sin\theta_{a}^{i} = \frac{x_{u}^{i} - x_{u,a}}{\sqrt{\left(x_{e}^{i} - x_{e,a}\right)^{2} + \left(x_{n}^{i} - x_{n,a}\right)^{2} + \left(x_{u}^{i} - x_{u,a}\right)^{2}}} = f^{i}\left(\mathbf{x}_{a}\right) \tag{4.63}$$

Table 4.6
Comparison for the Models and Estimation Algorithms Used for AOA-Based Positioning

{AU: Call out table sequentially in text}

Criterion	LSE	OVE	PLE
Type of solution	Iterative solution (requires refinement)	Closed-form (direct algebraic)	Closed-form (linearized LS)
Computational complexity	High (iterative matrix inversion, convergence required)	Moderate (matrix inversion required, but no iteration)	Low (simplified LS, minimal matrix operations)
Handling of nonlinearity	Solves nonlinear equations iteratively via Taylor series expansion	Uses vector-based formulation to preserve geometric relationships	Linearizes nonlinear AOA equations, introducing approximation errors
Robustness to noise	High (converges to best estimate under Gaussian noise)	Moderate (perpendicular fitting mitigates some noise effects)	Low (bias increases with noise, sensitive to outliers)
Accuracy	High (optimal under Gaussian noise)	Moderate to high (better than PLE, but still affected by bias)	Moderate (biased under high noise and poor geometry)
Initial guess required?	Yes (convergence depends on a good initial position)	No (direct computation)	No (direct computation)
Sensitivity to geometric configuration	High (convergence may fail if initial guess is poor or beacons are aligned)	Moderate (less sensitive than LSE but still geometry-dependent)	High (poor geometry causes large errors due to linearization effects)
Solution stability	Moderate (depends on iterative convergence, may be unstable for poor initial guesses)	High (closed-form and stable, but error grows with noise)	High (fast and repeatable, but biased)
Application scenarios	High-accuracy applications requiring precise positioning (e.g., indoor navigation, UWB localization)	Applications needing balance between computational efficiency and accuracy (e.g., sensor fusion, autonomous vehicles)	Real-time, low-computation environments where a fast but approximate solution is acceptable (e.g., initial positioning, quick AOA fixes)

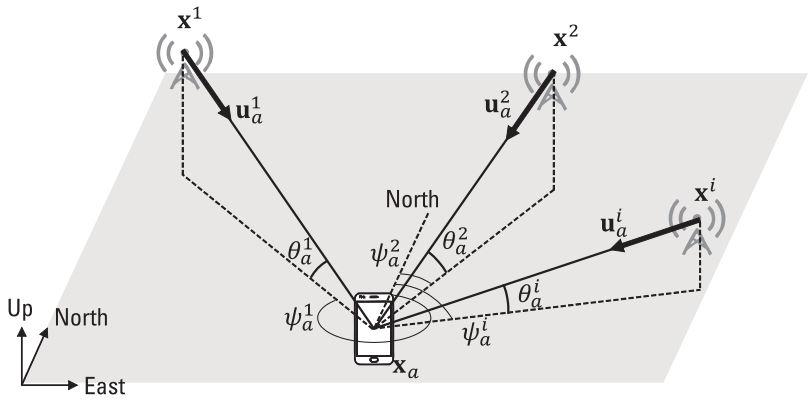

Figure 4.5 The measurements of AOA across the beacons.

$$\tan\psi_a^i = \frac{x_e^i - x_{e,a}}{x_n^i - x_{n,a}} = g^i\left(\mathbf{x}_a\right) \tag{4.64}$$

The measurement vector of each beacon $i = 1, \cdots, I$ can be formulated as

$$\mathbf{z}_a^i = \begin{bmatrix} \sin\theta_a^i \\ \tan\psi_a^i \end{bmatrix} \tag{4.65}$$

Incorporating the measurements from I beacons, the AOA measurement vector is defined as

$$\mathbf{z}_a = \begin{bmatrix} \mathbf{z}_a^1 \\ \vdots \\ \mathbf{z}_a^I \end{bmatrix} \tag{4.66}$$

Same as the direct range-based method, the state vector is defined in the form of (4.35). With the AOA measurements from multiple beacons, the agent position can be estimated by solving the geometry equations (4.63) and (4.64) for all I beacons. By applying the first-order Taylor series on (4.63), the trigonometric relationship can be rewritten as

$$\begin{aligned} f^i\left(\mathbf{x}_a\right) \approx f^i\left(\mathbf{x}_{a(0)}\right) &+ \frac{\partial f^i\left(\mathbf{x}_{a(0)}\right)}{\partial x_{e,a}}\delta x_{e,a} + \frac{\partial f^i\left(\mathbf{x}_{a(0)}\right)}{\partial x_{n,a}}\delta x_{n,a} \\ &+ \frac{\partial f^i\left(\mathbf{x}_{a(0)}\right)}{\partial x_{u,a}}\delta x_{u,a} \end{aligned} \tag{4.67}$$

where $\mathbf{X}_{a(0)}$ with the coordinate $(x_{e,a(0)}, x_{n,a(0)}, x_{u,a(0)})$ is the initial estimate of the agent's position, $\delta x_{e,a}$, $\delta x_{n,a}$, $\delta x_{u,a}$ are increments from the initial position to the next estimated agent position, the first-order partial derivative terms can be calculated as:

$$\frac{\partial f^i\left(\mathbf{x}_{a(0)}\right)}{\partial x_{e,a}} = \frac{\left(x_u^i - x_{u,a(0)}\right)\left(x_e^i - x_{e,a(0)}\right)}{\left[\left(x_e^i - x_{e,a(0)}\right)^2 + \left(x_n^i - x_{n,a(0)}\right)^2 + \left(x_u^i - x_{u,a(0)}\right)^2\right]^{3/2}} \tag{4.68}$$

$$\frac{\partial f^i\left(\mathbf{x}_{a(0)}\right)}{\partial x_{n,a}} = \frac{\left(x_u^i - x_{u,a(0)}\right)\left(x_n^i - x_{n,a(0)}\right)}{\left[\left(x_e^i - x_{e,a(0)}\right)^2 + \left(x_n^i - x_{n,a(0)}\right)^2 + \left(x_u^i - x_{u,a(0)}\right)^2\right]^{3/2}} \tag{4.69}$$

$$\frac{\partial f^i\left(\mathbf{x}_{a(0)}\right)}{\partial x_{u,a}} = \frac{-\left(x_e^i - x_{e,a(0)}\right)^2 - \left(x_n^i - x_{n,a(0)}\right)^2}{\left[\left(x_e^i - x_{e,a(0)}\right)^2 + \left(x_n^i - x_{n,a(0)}\right)^2 + \left(x_u^i - x_{u,a(0)}\right)^2\right]^{3/2}} \tag{4.70}$$

Similarly, the trigonometric relationship of the azimuth angle and the agent position can be applied with the first-order Taylor series expansion, in which (4.64) can be approximated by

$$g^i\left(\mathbf{x}_a\right) \approx g^i\left(\mathbf{x}_{a(0)}\right) + \frac{\partial g^i\left(\mathbf{x}_{a(0)}\right)}{\partial x_{e,a}}\partial x_{e,a} + \frac{\partial g^i\left(\mathbf{x}_{a(0)}\right)}{\partial x_{n,a}}\partial x_{n,a} + \frac{\partial g^i\left(\mathbf{x}_{a(0)}\right)}{\partial x_{u,a}}\partial x_{u,a} \tag{4.71}$$

$$\frac{\partial g^i\left(\mathbf{x}_{a(0)}\right)}{\partial x_{e,a}} = \frac{-1}{x_e^i - x_{e,a(0)}} \tag{4.72}$$

$$\frac{\partial g^i\left(\mathbf{x}_{a(0)}\right)}{\partial x_{n,a}} = \frac{x_e^i - x_{e,a(0)}}{\left(x_n^i - x_{n,a(0)}\right)^2} \tag{4.73}$$

$$\frac{\partial g^i\left(\mathbf{x}_{a(0)}\right)}{\partial x_{u,a}} = 0 \tag{4.74}$$

Based on the measurement vector and the state vector, the above relationships with I beacons can be represented as:

$$\mathbf{z}_a - \mathbf{z}_{a(0)} = \mathbf{H}_{a(0)} = \delta\mathbf{x}_a \tag{4.75}$$

$$\mathbf{H}_{a(0)} = \begin{bmatrix} \dfrac{\partial f^1(\mathbf{x}_{a(0)})}{\partial x_{e,a}} & \dfrac{\partial f^1(\mathbf{x}_{a(0)})}{\partial x_{n,a}} & \dfrac{\partial f^1(\mathbf{x}_{a(0)})}{\partial x_{u,a}} \\ \dfrac{\partial g^1(\mathbf{x}_{a(0)})}{\partial x_{e,a}} & \dfrac{\partial g^1(\mathbf{x}_{a(0)})}{\partial x_{n,a}} & 0 \\ \vdots & \vdots & \vdots \\ \dfrac{\partial f^1(\mathbf{x}_{a(0)})}{\partial x_{e,a}} & \dfrac{\partial f^1(\mathbf{x}_{a(0)})}{\partial x_{n,a}} & \dfrac{\partial f^1(\mathbf{x}_{a(0)})}{\partial x_{u,a}} \\ \dfrac{\partial g^1(\mathbf{x}_{a(0)})}{\partial x_{e,a}} & \dfrac{\partial g^1(\mathbf{x}_{a(0)})}{\partial x_{n,a}} & 0 \end{bmatrix} \tag{4.76}$$

Note that $\mathbf{z}_{a(0)}$ consisting of $\mathbf{z}^i_{a(0)} = [\, f^i(\mathbf{x}_{a(0)}) \;\; g^i(\mathbf{x}_{a(0)})]^{\mathrm{T}}$ is the approximate observation vector calculated based on the initial agent position $\mathbf{x}_{a(0)}$ with (4.63) and (4.64). To this step, we formed the linearized model between the AOA measurements and agent's state based on an initial guess. If the number of beacons is more than 3, then the estimation becomes an overdetermined problem. As mentioned earlier in this section, the noises of the measurements are assumed Gaussian random noise. Thus, the LSE can be achieved by

$$\delta\mathbf{x}_a = \left(\mathbf{H}_{a(0)}{}^{\mathrm{T}}\mathbf{H}_{a(0)}\right)^{-1}\mathbf{H}_{a(0)}{}^{\mathrm{T}}\delta\mathbf{z}_a \tag{4.77}$$

If the noise standard deviations are available, the WLS estimation can be conducted to achieve a MLE.

$$\delta\mathbf{x}_a = \left(\mathbf{H}_{a(0)}{}^{\mathrm{T}}\mathbf{W}_a\mathbf{H}_{a(0)}\right)^{-1}\mathbf{H}_{a(0)}{}^{\mathrm{T}}\mathbf{W}_a\delta\mathbf{z}_a$$

$$\mathbf{W}_a = \begin{bmatrix} \left(\sigma^2_{f^1(\mathbf{x}_{a(0)})}\right)^{-1} & 0 & \cdots & 0 & 0 \\ 0 & \left(\sigma^2_{g^1(\mathbf{x}_{a(0)})}\right)^{-1} & \cdots & 0 & 0 \\ \vdots & \vdots & \ddots & \vdots & \vdots \\ 0 & 0 & \cdots & \left(\sigma^2_{f^1(\mathbf{x}_{a(0)})}\right)^{-1} & 0 \\ 0 & 0 & \cdots & 0 & \left(\sigma^2_{g^1(\mathbf{x}_{a(0)})}\right)^{-1} \end{bmatrix} \tag{4.78}$$

where $\sigma^2_{f^1(\mathbf{x}_{a(0)})}$ and $\sigma^2_{g^1(\mathbf{x}_{a(0)})}$ representing the variance of the AOA measurements corresponding to the elevation angle and the azimuth angle, respectively.

However, the derived equation (4.64) becomes unstable when the azimuth angle ψ is 90° or 270°, resulting in singular points in the measurement model. This issue arises because the denominator in the azimuth angle equation approaches 0, leading to numerical instability. In practice, 90° AOA measurements are common. For example, if the agent is positioned directly East of the beacon, the azimuth angle is $\psi = 90°$, creating a singularity in the Jacobian matrix. To overcome this issue, spatial rotations in 3-D space can be parametrized using unit quaternions. Quaternions provide a 4-D representation of 3-D rotations, avoiding the singularities that occur in Euler angle-based formulations. The derivation of this approach can be found in [60], and the corresponding Jacobian matrix remains the same as in (4.76). It is important to note that the derivation of quaternion-based transformations can be mathematically complex. However, it effectively eliminates singularities and ensures stability in AOA-based positioning models.

4.4.2 Model and Estimation: OVE

The OVE is a closed-form solution for estimating an agent's position using AOA measurements from multiple beacons. Unlike LSE, which requires iterative refinement, OVE formulates the localization problem as a linear system and provides a direct algebraic solution.

OVE is called "orthogonal" because it minimizes perpendicular distance errors between the estimated agent location and the bearing vectors. The method assumes that the true agent position lies along the intersection of bearing lines, but due to noise, the actual intersection is imperfect. OVE computes the best-fit location by solving for the agent's position in an LS sense.

Let's start with the measurement model in OVE, it uses unit direction vector representation. Similar to LSE, each beacon i measures the elevation angles θ^i_a and the azimuth angles ψ^i_a of the agent's position. These angles define a unit direction vector from beacon i to the agent, as

$$\boldsymbol{\eta}^i_a = \begin{bmatrix} \cos\theta^i_a \sin\psi^i_a \\ \cos\theta^i_a \cos\psi^i_a \\ \sin\theta^i_a \end{bmatrix} \tag{4.79}$$

The true agent position $\mathbf{x}_a$, as defined by (4.15) in the ENU coordinate, must lie along the bearing line defined by each beacon. This relationship can be expressed as:

$$\mathbf{x}_a = \mathbf{x}^i + \lambda_i \eta_a^i \tag{4.80}$$

where $\mathbf{x}^i$ is the known coordinate of the beacon at (x_e^i, x_n^i, x_u^i), and λ_i is an unknown scaling factor, representing the agent's distance from the beacon. It defines a ray in 3-D space. As two skew lines in 3-D do not intersect (only if in the same plane), measurements (i.e., line of ray) from at $I \geq 3$ beacons are needed to obtain an exact intersection indicating the agent's location, or forms an overdetermined system to be solved by LS.

To derive a linear system for positioning, a popular approach is multiplying a unit vector $\mathbf{s}_a^i$ orthogonal to η_a^i on both sides to eliminate the distance factor, giving

$$\mathbf{s}_a^{i\,\mathrm{T}} \mathbf{x}_a = \mathbf{s}_a^{i\,\mathrm{T}} \mathbf{x}^i \tag{4.81}$$

where $\mathbf{s}_a^i \cdot \eta_a^i = 0$ (orthogonal vectors), $\|\mathbf{s}_a^i\| = 1$ (unit vector), and the superscript T denotes the transpose of a vector. A straightforward candidate of η_a^i is to rotate $\mathbf{s}_a^i$ with 90° in terms of its related angular parameter, that is, increasing θ_a^i by $\pi/2$ gives

$$\mathbf{s}_a^i = \begin{bmatrix} \cos\left(\theta_a^i + \dfrac{\pi}{2}\right)\sin\psi_a^i \\ \cos\left(\theta_a^i + \dfrac{\pi}{2}\right)\cos\psi_a^i \\ \sin\left(\theta_a^i + \dfrac{\pi}{2}\right) \end{bmatrix} = \begin{bmatrix} -\sin\theta_a^i \sin\psi_a^i \\ -\sin\theta_a^i \cos\psi_a^i \\ \cos\theta_a^i \end{bmatrix} \tag{4.82}$$

Thus, for each beacon, the geometrical relationship from (4.81) can be rewritten as

$$\begin{aligned} &-\sin\theta_a^i \sin\psi_a^i x_{e,a} - \sin\theta_a^i \cos\psi_a^i x_{n,a} + \cos\theta_a^i x_{u,a} \\ &= -\sin\theta_a^i \sin\psi_a^i x_e^i - \sin\theta_a^i \cos\psi_a^i x_n^i + \cos\theta_a^i x_u^i \end{aligned} \tag{4.83}$$

$$\underbrace{\begin{bmatrix} -\sin\theta_a^1 \sin\psi_a^1 & -\sin\theta_a^1 \cos\psi_a^1 & \cos\theta_a^1 \\ -\sin\theta_a^2 \sin\psi_a^2 & -\sin\theta_a^2 \cos\psi_a^2 & \cos\theta_a^2 \\ \vdots & \vdots & \vdots \\ -\sin\theta_a^I \sin\psi_a^I & -\sin\theta_a^I \cos\psi_a^I & \cos\theta_a^I \end{bmatrix}}_{\mathbf{s}_a} \begin{bmatrix} x_{e,a} \\ x_{n,a} \\ x_{u,a} \end{bmatrix}$$

$$= \underbrace{\begin{bmatrix} -\sin\theta_a^1 \sin\psi_a^1 x_e^1 - \sin\theta_a^1 \cos\psi_a^1 x_n^1 + \cos\theta_a^1 x_u^1 \\ -\sin\theta_a^2 \sin\psi_a^2 x_e^2 - \sin\theta_a^2 \cos\psi_a^2 x_n^2 + \cos\theta_a^2 x_u^2 \\ \vdots \\ -\sin\theta_a^I \sin\psi_a^I x_e^I - \sin\theta_a^I \cos\psi_a^I x_n^I + \cos\theta_a^I x_u^I \end{bmatrix}}_{\mathbf{z}_a} \tag{4.84}$$

which forms a linear equation associating the AOA measurements and the location of the agent. By collecting the linear equations from all beacons, the geometrical relationship can be established in a matrix form, as follows.

Similar to the preceding overdetermined problem, the agent's position can be resolved by an LSE, using

$$\mathbf{x}_a = \left(\mathbf{S}_a^{\mathrm{T}} \mathbf{S}_a\right)^{-1} \mathbf{S}_a^{\mathrm{T}} \mathbf{z}_a \tag{4.85}$$

which provides the closed-form 3-D positioning solution with OVE. Note that OVE is derived by transforming the nonlinear relationship in a linear manner, which inherits a bias during the estimation. Specifically, because $\mathbf{S}_a$ depends on the AOA measurements (θ and ψ) with noises, it is also correlated with the noise in $\mathbf{z}_a$, making OVE a biased estimator [56]. This bias is generally related to the measurement noise covariance as well as the scale of the ranging measurement. For example, if the agent is very far from the beacons, small angular errors would lead to large position errors, and the linear approximation mislocates the intersection systematically.

4.4.3 Model and Estimation: 3-D PLE

Considering the 2-D (in the horizontal East-North plane) position estimation based on AOA measurements, the objective is to search for an agent position that minimizes the error compared to each beacon's AOA measurements according to the geometrical relationship in (4.80). A straightforward approach is the PLE, which establishes linear equations based on the geometrical relationship between angular measurements and the agent's location and solves the equations from all available beacons. More specifically, the geometrical relationship can be described in terms of East and North directions, respectively, as follows:

$$x_{e,a} - x_e^i = \lambda_i \sin\psi_a^i \tag{4.86}$$

$$x_{n,a} - x_n^i = \lambda_i \cos\psi_a^i \tag{4.87}$$

If $\cos\psi_a^i \neq 0$, the unknown distance λ_i in (4.87) can be substituted by the relationship in (4.86), yielding

$$x_{n,a} - x_n^i = \frac{x_{e,a} - x_e^i}{\sin\psi_a^i}\cos\psi_a^i \tag{4.88}$$

By multiplying $\sin\psi_a^i$ on both sides, the angular relationship can be rewritten as

$$\cos\psi_a^i x_{e,a} - \sin\psi_a^i x_{n,a} = \cos\psi_a^i x_e^i - \sin\psi_a^i x_n^i \tag{4.89}$$

which represents the line of bearing in Cartesian form. It is essentially the equation of a line passing through (x_e^i, x_n^i) with a normal vector $(-\cos\psi_a^i, \sin\psi_a^i)$. We can verify that this equation is satisfied by any point $(x_{e,a}, x_{e,a})$ that lies on the line of bearing. Thus, each AOA measurement provides one linear equation of the form (4.89) relating $x_{e,a}$ and $x_{n,a}$, which can be combined to form a linear system:

$$\underbrace{\begin{bmatrix} \cos\psi_a^1 & -\sin\psi_a^1 \\ \cos\psi_a^2 & -\sin\psi_a^2 \\ \vdots & \vdots \\ \cos\psi_a^I & -\sin\psi_a^I \end{bmatrix}}_{\mathbf{S}_a} \begin{bmatrix} x_{e,a} \\ x_{n,a} \end{bmatrix} = \underbrace{\begin{bmatrix} \cos\psi_a^1 x_e^1 - \sin\psi_a^1 x_n^1 \\ \cos\psi_a^2 x_e^2 - \sin\psi_a^2 x_n^2 \\ \vdots \\ \cos\psi_a^I x_e^I - \sin\psi_a^I x_n^I \end{bmatrix}}_{\mathbf{z}_a} \tag{4.90}$$

If $I = 2$ and the two lines are not parallel, this system has an exact solution (the intersection point). With $I > 2$, the system is overdetermined (more equations than unknowns), and an exact solution generally does not exist due to the noise causing inconsistency. In that case, we seek an LS solution that minimizes the sum of squared errors, which yields the positioning solution as

$$\begin{bmatrix} x_{e,a} \\ x_{n,a} \end{bmatrix} = \left(\mathbf{S}_a^{\mathrm{T}}\mathbf{S}_a\right)^{-1}\mathbf{S}_a^{\mathrm{T}}\mathbf{z}_a \tag{4.91}$$

When the localization is in 3-D, one straightforward extension of the PLE is to decouple the problem into horizontal and vertical components [57]. The idea is to first estimate the East-North coordinates using only the azimuth angles (ignoring elevation) and then estimate the Up coordinate using

the elevation angles and the previously estimated horizontal position, namely the 3-D PLE.

For the horizontal position, by ignoring the elevation angle θ_a^i, each beacon provides an azimuth angle ψ_a^i, while the agent's position is projected at $(x_{e,a}, x_{n,a})$ on the horizontal plane. Thus, the 3-D estimation problem is reduced into 2-D, which can be solved by the preceding PLE using (4.90).

The second step is to estimate the Up coordinate based on the horizontal positioning solution and the elevation angle measurement θ_a^i from each beacon. Considering the geometry for a given beacon i, the elevation relates the difference in height to the horizontal distance from the beacon, which can be described by a tangent function:

$$\tan\theta_a^i = \frac{x_u^i - x_{u,a}}{\sqrt{\left(x_e^i - x_{e,a}\right)^2 + \left(x_n^i - x_{n,a}\right)^2}} \tag{4.92}$$

where the Up coordinate can be estimated by a specific beacon's measurement, using

$$x_{u,a}^i = x_u^i - \tan\theta_a^i \sqrt{\left(x_e^i - x_{e,a}\right)^2 + \left(x_n^i - x_{n,a}\right)^2} \tag{4.93}$$

or generally

$$x_{u,a}^i = x_u^i - \left\|\mathbf{x}_a(1:2) - \mathbf{x}^i(1:2)\right\| \tan\theta_a^i \tag{4.94}$$

where $x_{u,a}^i$ is the Up coordinate estimation from the measurement of beacon i, the bracket (1:2) denotes the vector only incorporating the first and second entries (East and North). Due to the measurement noise, the estimation results from different beacons may not be consistent. Thus, a sensible approach is to average these to reduce the effect of noise, using

$$x_{u,a} = \frac{1}{I}\sum_{i=1}^{I}\left(x_u^i - \left\|\mathbf{x}_a(1:2) - \mathbf{x}^i(1:2)\right\| \tan\theta_a^i\right) \tag{4.95}$$

By combining $x_{u,a}$ with the preceding estimated $x_{e,a}$ and $x_{n,a}$ from the first step, the 3-D positioning solution for the agent can be obtained. In many cases, if the noise is not too large, $x_{u,a}^i$ will not vary drastically with i, so the average is reasonable. One could also incorporate a weighted average approach (e.g., giving more weight to measurements from closer receivers, which tend to have more accurate elevation information), if the measurement quality is known.

Note that the 2-D PLE solution could be significantly biased, especially in the case with large bearing noise or unfavorable geometry. The reason is that the linear equation (4.89) was derived by effectively treating ψ_a^i as exact when forming $\mathbf{S}_a$ and $\mathbf{z}_a$, thereby "pushing" the nonlinearity into the error term. In other words, we replaced the true nonlinear measurement equation related to ψ_a^i with an arctangent function, with a linear equation plus an approximation error. A certain bias is introduced depending on the bearing noise variance and the target-to-sensor geometry. Thus, the 3-D PLE solution also inherits the same bias issue as the 2-D PLE for the horizontal part, and the subsequent averaging for $x_{u,a}$ can introduce an additional error if the estimation of ($x_{e,a}$, $x_{n,a}$) is biased or if the geometry varies significantly among the measurements. Nonetheless, the PLE is attractive for its simplicity and often serves as an initial guess for more advanced iterative algorithms (such as Gauss-Newton or EKFs), but sacrifices accuracy for computational efficiency. While it is widely used in real-time applications, it suffers from bias and sensitivity to noise.

4.5 Challenges for Radio Signal-Based Indoor Positioning

Looking at (4.20), the factors affecting the accuracy of estimation can be separated into two groups, the qualities of the measurement vector $\mathbf{z}_a$ and the linearized measurement model matrix $\mathbf{H}_a$. The next two subsections discuss the quality of the measurement and the two subsections after that discuss the quality of the model.

4.5.1 Thermal Noise on the Oscillator

Accurate positioning using TDOA and AOA methods relies on precise time and phase measurements. Because oscillators serve as the time-keeping elements in wireless devices, their stability directly affects the accuracy of these positioning techniques. However, real-world oscillators are subject to thermal noise, leading to random fluctuations in their frequency and phase over time. These variations introduce timing uncertainty, which degrades the precision of TDOA measurements and, in some cases, impacts multidevice AOA estimations.

Before considering the effects of noise, oscillators undergo calibration to correct their initial frequency offset. This process aligns the oscillator's frequency to a reference standard, reducing systematic errors. However, calibration alone cannot eliminate random frequency fluctuations, which persist due to the fundamental physical limitations of the oscillator. Even a well-calibrated

oscillator exhibits phase noise and frequency noise, which introduce small, unpredictable errors in the timing of received signals. These residual noise components are particularly problematic in TDOA systems, where even nanosecond-level timing errors translate to substantial localization inaccuracies.

In the context of RF-based positioning, phase noise refers to short-term random variations in the phase of an oscillator's output signal. It is commonly represented in the frequency domain as a power spectral density (PSD), denoted as $S_{c\phi}(f)$, which quantifies how the oscillator's phase stability degrades at different frequency offsets. These phase fluctuations manifest as timing jitter in the time domain, causing slight variations in when signal peaks and zero-crossings occur. Because TDOA positioning depends on precise timestamps, any timing jitter can lead to errors in distance estimation.

Similarly, frequency noise describes small, random deviations in the oscillator's output frequency over time. These deviations accumulate and cause the oscillator to drift slightly away from its nominal frequency. Frequency noise and phase noise are closely related—phase noise is essentially the integral of frequency noise over time, meaning that frequency instability leads to increased phase uncertainty as time progresses.

The random nature of these noise sources can be mathematically modeled using a state-space representation of oscillator drift. The time-offset error and its rate of change (drift) evolve over time according to the following process noise covariance matrix:

$$\mathbf{Q}_{\text{clock}} = \begin{bmatrix} S_{c\phi}\tau + \frac{1}{3}S_{cf}\tau^3 & \frac{1}{2}S_{cf}\tau^2 \\ \frac{1}{2}S_{cf}\tau^2 & S_{cf}\tau \end{bmatrix}, \begin{cases} S_{c\phi} = c^2 \cdot \frac{h_0}{2} \\ S_{cf} = c^2 \cdot 2\pi^2 \cdot h_{-2} \end{cases} \tag{4.96}$$

where τ is the update interval, $S_{c\phi}$ is the oscillator phase noise PSD, and S_{cf} is the oscillator frequency noise PSD. The first and second rows are corresponding to the time offset and its drift, respectively. According to [58], the coefficients of the TCXO are $h_0 = 2 \times 10^{-19}$ and $h_{-2} = 2 \times 10^{-20}$. If manufacturer-provided oscillator noise specifications are available, these values should be substituted to ensure an accurate system model.

The presence of oscillator noise affects positioning accuracy in several ways:

1. *TDOA sensitivity to timing errors:* In TDOA systems, each receiver's clock must be synchronized to the nanosecond level. Any oscillator-induced timing jitter directly translates to range estimation errors. For

instance, a 1-ns timing uncertainty causes a 30-cm error in range calculations, as radio waves travel approximately 0.3m per nanosecond. If the oscillator exhibits significant phase noise, these errors accumulate over multiple measurements, reducing overall localization precision.

2. *AOA impact in multidevice systems:* While single-device AOA measurements (e.g., an antenna array on a single receiver) are not directly impacted by absolute oscillator drift, multireceiver AOA systems or TDOA-AOA hybrid systems rely on synchronized phase references across multiple nodes. In such cases, oscillator phase noise introduces drift between receivers, causing angle estimation errors that propagate into position calculations.
3. *Long-term drift and synchronization requirements:* Even if a system starts with well-calibrated oscillators, long-term drift can cause increasing timing discrepancies. High-precision systems must periodically resynchronize oscillators using external references, such as GPSDOs or common-view time transfer techniques. If synchronization updates are infrequent, the accumulated phase noise may exceed acceptable error thresholds.

To minimize the impact of oscillator noise on TDOA/AOA positioning, several mitigation techniques can be employed:

- *High-stability oscillators:* Using low-phase-noise oscillators such as oven-controlled crystal oscillators (OCXOs) or atomic clocks significantly reduces timing uncertainty. However, these components increase cost and power consumption.
- *Frequent synchronization:* Periodic clock synchronization (e.g., through over-the-air timing beacons) helps to correct drift before it degrades positioning accuracy.
- *Adaptive filtering:* Advanced filtering techniques, such as EKF, incorporate oscillator noise models to compensate for timing errors dynamically. These methods are particularly useful when oscillator noise characteristics are well understood and can be modeled accurately.
- *Dual-frequency compensation:* Some positioning systems use dual-frequency signals to estimate and correct oscillator drift in real time.

4.5.2 Multipath and NLOS Effects

TDOA and AOA rely on the assumption that signals travel in a straight-line, LOS path between the transmitter and the receiver. However, in realistic

environments, obstacles such as walls, buildings, and furniture cause the transmitted signal to reflect, diffract, or scatter, resulting in multipath propagation. In some cases, the direct LOS path is completely obstructed, leading to NLOS reception, where only reflected or diffracted signals reach the receiver.

These propagation effects introduce significant errors in positioning calculations. As illustrated in Figure 4.6, multipath propagation causes multiple signal copies to arrive at the receiver at different times, distorting ranging and angle measurements. In NLOS scenarios, the absence of the direct path results in systematic biases in estimated distances and angles. These errors increase the uncertainty of position estimation and degrade the overall accuracy of TDOA and AOA-based localization systems.

This section discusses the challenges posed by multipath and NLOS propagation, followed by two common mitigation approaches: channel estimation and ray tracing-based modeling.

4.5.2.1 Impact on TDOA and AOA Positioning

TDOA-based positioning estimates a signal source's location by measuring the TDOA between multiple receivers. However, multipath and NLOS conditions disrupt these measurements in different ways:

- *Multipath effects:* When a signal travels via multiple paths (direct and reflected), the receiver might detect multiple arrival peaks in the received waveform. The TDOA algorithm may lock onto the wrong peak, leading to incorrect time differences and a shifted position estimate.

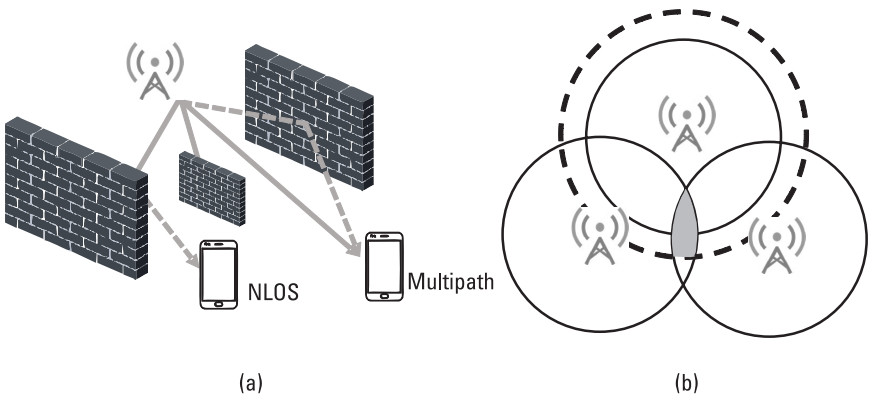

Figure 4.6 (Left) Multipath and NLOS. (Right) How the reflection affects the positioning trilateration.

- *NLOS effects:* If the direct path is blocked, the receiver only detects reflected signals. Because these reflections travel a longer path than the true LOS signal, the measured arrival time is delayed, introducing a positive bias in the estimated distance. This leads to an overestimation of range differences, which distorts the computed hyperbolic position solution. For example, in an indoor environment, a TDOA-based system may estimate a transmitter's position to be tens or even hundreds of meters away from its actual location due to NLOS propagation errors.

AOA-based positioning systems estimate the transmitter's location by measuring the angle at which a signal arrives at multiple receivers equipped with antenna arrays. However, multipath and NLOS introduce errors in direction estimation:

- *Multipath effects:* When a receiver detects both direct and reflected signals, its AOA algorithm might be confused by multiple arriving directions. If the strongest received signal is a reflection, the system may incorrectly infer that the transmitter is located in the wrong direction.
- *NLOS effects:* In pure NLOS conditions, the direct path is completely blocked, and the receiver only detects reflected signals. Consequently, the estimated arrival angle corresponds to the direction of the reflecting surface rather than the true transmitter location.

In urban and indoor environments, AOA errors due to NLOS can result in severe mislocalization, as signals might appear to originate from walls or objects rather than the actual source.

4.5.2.2 Channel Estimation for Multipath Mitigation

One approach to mitigating multipath effects is channel estimation, which involves analyzing the channel impulse response (CIR) to separate direct and reflected signal components. This method is embedded within the receiver's signal processing algorithms. The idea is to estimate the "channels," which means the signal paths from a beacon to an agent's receiver. As a standard form of the received multipath signal, consider that one channel of the LOS path and the $M-1$ channel of multipaths can be written as

{AU: Edits correct?}

$$s(t)=\sum_{m=0}^{M-1} a_m e^{-j\phi_m} r\left(t-\tau_m\right) \tag{4.97}$$

where a_m and ϕ_m are the amplitude and phase of the m^{th} signal propagation path, τ_m is the corresponding propagation delay, and $r(t)$ is the transmitted

signal. By correlating the received signal s with the local signal replica of r, the time delay τ and the phase angle ϕ of the $M-1$ multipath channels can be estimated using

$$\left(\hat{\tau},\hat{\phi}\right) = \underset{\tau,\phi}{\arg\max}\ \text{correlation}\left(s, r\left(\tau,\phi\right)\right) \tag{4.98}$$

where the hat denotes the estimated variable. The first detected peak in the estimated channel impulse response typically corresponds to the LOS path (if present), while later peaks represent multipath components. Advanced methods such as the MLE and multipath estimating delay lock loop (MEDLL) refine these estimates to enhance accuracy. A review of various channel estimation techniques for multipath mitigation is available in [59]. Although channel estimation can help to identify early-arriving signal components (which are likely LOS), it does not always eliminate NLOS bias. If the direct path is completely blocked, the earliest detected signal will still be an indirect reflection, leading to unavoidable positioning errors.

4.5.3 Distribution of Beacons

A couple of the most frequently asked questions of setting up a beacon-based indoor positioning system are: Where should I place the beacons? Does the location of beacons affect the performance of my indoor positioning system? Intuitively, the answer is yes, but the real question is how to quantify this relationship. This section aims to answer this question. Considering the TOA and TDOA-based point positioning methods, both methods can form a state and measurement equation as follows:

$$\mathbf{x}_a = \left(\mathbf{H}_a{}^{\mathrm{T}}\mathbf{H}_a\right)^{-1}\mathbf{H}_a{}^{\mathrm{T}}\mathbf{z}_a \tag{4.99}$$

As shown in (4.99), the state $\mathbf{x}_a$ is estimated by two factors: (1) the quality of the measurements, $\mathbf{z}_a$ and (2) the LOS vectors from beacons relative to the agent a, $\mathbf{H}_a$ which assumes a linear relationship. To theoretically derive their quantitative impacts, the following analysis is used. If there is an random noise $\omega_{\mathbf{z}_a}$ in the measurement vector where each component follows a zero mean Gaussian distribution $\mathcal{N}(0, \sigma^2_{\mathbf{z}_a})$, it will also result in a zero mean Gaussian random noise $\omega_{\mathbf{x}_a}$ in the state estimation, in which $\omega_{\mathbf{x}_a} = (\mathbf{H}_a{}^{\mathrm{T}}\mathbf{H}_a)^{-1}\mathbf{H}_a{}^{\mathrm{T}}\omega_{\mathbf{z}_a}$. Then the noise covariance of the state $\mathbf{C}(\mathbf{x}_a)$ is calculated as

$$\mathbf{C}\left(\mathbf{x}_a\right) = \mathbb{E}\left[\omega_{\mathbf{x}_a}\omega_{\mathbf{x}_a}{}^{\mathrm{T}}\right] \tag{4.100}$$

where $\mathbb{E}[\cdot]$ denotes the expectation calculation. To substitute the state estimation noise $\omega_{\mathbf{x}_a}$ with the linear relationship, we obtain,

$$\begin{aligned}\mathbf{C}(\mathbf{x}_a) &= \mathbb{E}\left[\mathbf{K}\omega_{\mathbf{z}_a}\left(\mathbf{K}\omega_{\mathbf{z}_a}\right)^{\mathrm{T}}\right] \\ &= \mathbb{E}\left[\left(\mathbf{H}_a{}^{\mathrm{T}}\mathbf{H}_a\right)^{-1}\mathbf{H}_a{}^{\mathrm{T}}\omega_{\mathbf{z}_a}\omega_{\mathbf{z}_a}{}^{\mathrm{T}}\mathbf{H}_a\left(\mathbf{H}_a{}^{\mathrm{T}}\mathbf{H}_a\right)^{-1}\right] \\ &= \left(\mathbf{H}_a{}^{\mathrm{T}}\mathbf{H}_a\right)^{-1}\mathbf{H}_a{}^{\mathrm{T}}\mathbf{C}(\mathbf{z}_a)\mathbf{H}_a\left(\mathbf{H}_a{}^{\mathrm{T}}\mathbf{H}_a\right)^{-1} \\ \text{where } \mathbf{K} &= \left(\mathbf{H}_a{}^{\mathrm{T}}\mathbf{H}_a\right)^{-1}\mathbf{H}_a{}^{\mathrm{T}}\end{aligned} \tag{4.101}$$

Assuming that $\mathbf{z}_a$ are i.i.d. (independent and identically distributed) random variables, the noise covariance of measurement vector $\mathbf{z}_a$ becomes

{AU: Is this the correct equation? Do you mean (4.77)?}

$$\mathbf{C}(\mathbf{z}_a) = \mathbf{I}\cdot\sigma^2_{\mathbf{z}_a} \tag{4.102}$$

where $\mathbf{I}$ denotes identity matrix. Then (3.77) becomes

$$\mathbf{C}(\mathbf{x}_a) = \left(\mathbf{H}_a{}^{\mathrm{T}}\mathbf{H}_a\right)^{-1}\sigma^2_{\mathbf{z}_a} \tag{4.103}$$

As can be seen, the noise covariance becomes only related to a standardized measurement noise $\sigma^2_{\mathbf{z}_a}$ and $(\mathbf{H}_a{}^{\mathrm{T}}\mathbf{H}_a)^{-1}$. For ranging-based measurements, general speaking, the state vector is $\mathbf{x}_a = [x_{e,a} \quad x_{n,a} \quad x_{u,a}]^T$. Recall that the $\mathbf{C}(\mathbf{x}_a)$ indicates the covariance between each pair of elements in the East, North, and up directions. Then the overall variance of the state estimation in the NED coordinate can be approximated by the sum of its variances in each directions, using

$$\begin{aligned}\sigma^2_{x_{\mathrm{enu},a}} &= \sigma^2_{x_{e,a}} + \sigma^2_{x_{n,a}} + \sigma^2_{x_{u,a}} \\ \sigma_{x_{\mathrm{enu},a}} &= \sqrt{\sigma^2_{x_{e,a}} + \sigma^2_{x_{n,a}} + \sigma^2_{x_{u,a}}} = \sqrt{\mathrm{tr}\left(\mathbf{C}(\mathbf{x}_a)\right)}\end{aligned} \tag{4.104}$$

where tr(·) denotes the trace of a square matrix that sums the elements on the main diagonal. Substituting (4.102) to (4.103),

$$\sigma_{x_{\mathrm{enu},a}} = \sqrt{\mathrm{tr}\left(\left(\mathbf{H}_a{}^{\mathrm{T}}\mathbf{H}_a\right)^{-1}\sigma^2_{\mathbf{z}_a}\right)} = \sqrt{\mathrm{tr}\left(\left(\mathbf{H}_a{}^{\mathrm{T}}\mathbf{H}_a\right)^{-1}\right)}\cdot\sigma_{\mathbf{z}_a} \tag{4.105}$$

For the simplicity, we describe the components in $(\mathbf{H}_a{}^{\mathrm{T}}\mathbf{H}_a)^{-1}$ as follows:

$$\left(\mathbf{H}_a^{\mathrm{T}}\mathbf{H}_a\right)^{-1} = \begin{bmatrix} \kappa_{x_e x_e} & \kappa_{x_e x_n} & \kappa_{x_e x_u} \\ \kappa_{x_n x_e} & \kappa_{x_n x_n} & \kappa_{x_n x_u} \\ \kappa_{x_u x_e} & \kappa_{x_u x_n} & \kappa_{x_u x_u} \end{bmatrix} \tag{4.106}$$

Then

$$\sigma_{x_{\mathrm{enu},a}} = \sqrt{\kappa_{x_e x_e} + \kappa_{x_n x_n} + \kappa_{x_u x_u}} \cdot \sigma_{\mathbf{z}_a} \tag{4.107}$$

Considering (4.107), if $\sqrt{\kappa_{x_e x_e} + \kappa_{x_n x_n} + \kappa_{x_u x_u}}$ equals κ, then 1m of standardized measurement noise will produce $\kappa \times 1$m of the positioning noise. In the GNSS field, $\sqrt{\kappa_{x_e x_e} + \kappa_{x_n x_n} + \kappa_{x_u x_u}}$ is well-known as dilution of precision (DOP) as the DOP factor will dilute (transform the domain of) the measurement uncertainty into the positioning uncertainty This book also adopts the same logic and calls it DOP. Analogous to (4.104), the DOP can be divided based on the direction of the state concerned.

$$\begin{aligned} \sigma_{x_{\mathrm{horizontal},a}} &= \sqrt{\sigma^2_{x_{e,a}} + \sigma^2_{x_{n,a}}} = \sqrt{\kappa_{x_e x_e} + \kappa_{x_n x_n}} \cdot \sigma_{\mathbf{z}_a} = HDOP \cdot \sigma_{\mathbf{z}_a} \\ \sigma_{x_{\mathrm{vertical,a}}} &= \sqrt{\sigma^2_{x_{u,a}}} = \sqrt{\kappa_{x_u x_u}} \cdot \sigma_{\mathbf{z}_a} = VDOP \cdot \sigma_{\mathbf{z}_a} \end{aligned} \tag{4.108}$$

HDOP and *VDOP* are therefore used to indicate that 1m of measurement error will be diluted (mapped) to the positioning error in the horizontal and vertical directions, respectively. Thus, the smaller the *HDOP* and *VDOP* are, the less affected the positioning result will be by the measurement errors. The immediate next issue is how to make them smaller.

{AU: Edits correct?}

The DOP is calculated based on the measurement matrix $\mathbf{H}_a$. Taking TOA as an example, $\mathbf{H}_a = [\mathbf{h}_a^1 \ \cdots \ \mathbf{h}_a^i \ \cdots \ \mathbf{h}_a^J]^T$ and $\mathbf{h}_a^i$ denotes the unit LOS vector between the beacon i and the agent a. This indicates that the distribution of the beacons related to the agents is very related to the DOP. This idea can be easily understood by referring to the illustration given in Figure 4.7.

To echo back to the question mentioned in the beginning of this section, the simulation of placing the beacons at different locations can be achieved by using (4.108). Zwirello et al. [60] analyzed the change of HDOP and VDOP using different distributions of beacons as shown in Figure 4.8. As can be seen, the DOP values changes as the change of the agent receiver's location. In the other words, based on a predefined distribution of beacons, some areas could have larger DOP than others. Readers should aware this in designing a beacon-based indoor positioning system.

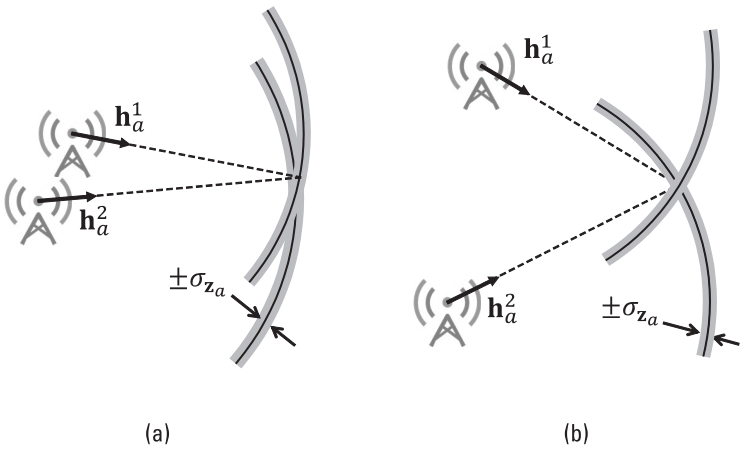

Figure 4.7 Beacon distributions with: (left) a higher DOP, and (right) a lower DOP.

The discussion in this section can apply to not only the TOA ranging and RSS ranging-based point positioning method but also to the TDOA-ranging and AOA-based methods by simply replacing the measurement matrix $\mathbf{H}_a$.

4.5.4 Nonlinearity Caused by an Initial Guess

In this chapter, we have assumed the iterative least squares (ILS) estimation can successfully solve the agent receiver's position based on a major assumption; the initial guess of the state, $\mathbf{x}_{a(0)}$, is sufficiently close to the actual position of the agent, $\mathbf{x}_{gt,a}$. This assumption is critical because ILS relies on a linearized measurement model, which only holds when the estimated position is near the true location. Figure 4.9 shows the importance of this assumption. As can be seen, if the initial guess is not accurate enough, the assumption $\mathbf{h}^i_{a(0)} \approx \mathbf{h}^i_{gt,a}$ cannot be made. If the distance between the initial guess and the ground truth location of the agent is relatively small compared to the distance between the beacons to the agent, the assumption can still hold. In the other words, the required accuracy of the initial guess to solve the point-positioning methods is related to the size of the indoor venue of a designed indoor positioning system.

However, the radio-signal based point positioning also plays a role to provide initial guess for some multisensor integrated indoor positioning systems. Thus, the stringent requirement on the initial guess may not be appropriate to those systems. An alternative solution is to consider higher-order terms when

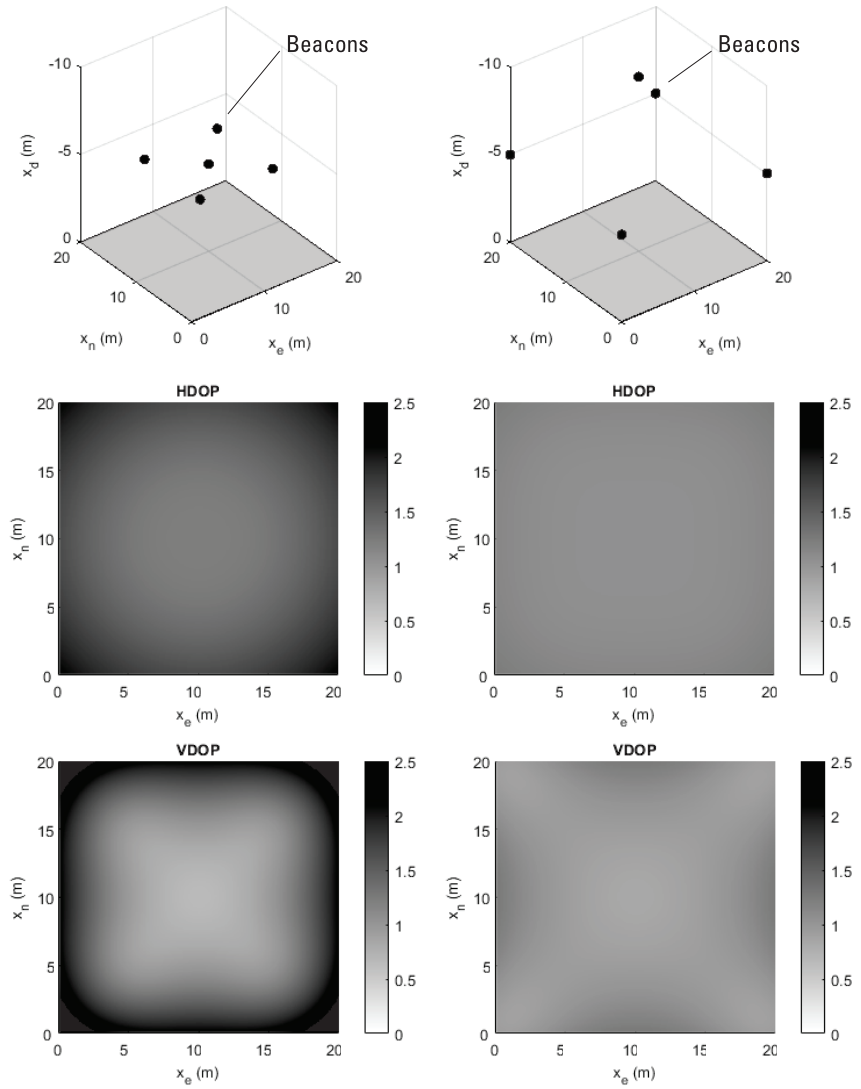

Figure 4.8 HDOPs and VDOPs under different beacon distributions [60].

linearizing the measurement models. The higher-order terms are usually used to describe the model with higher nonlinearity. As shown in (4.16) and (4.36), the TOA and TDOA measurement models are nonlinear. Taking the TOA one as an example, if we consider a second-order term in the linearization via Taylor series expansion, the linearized measurement model becomes:

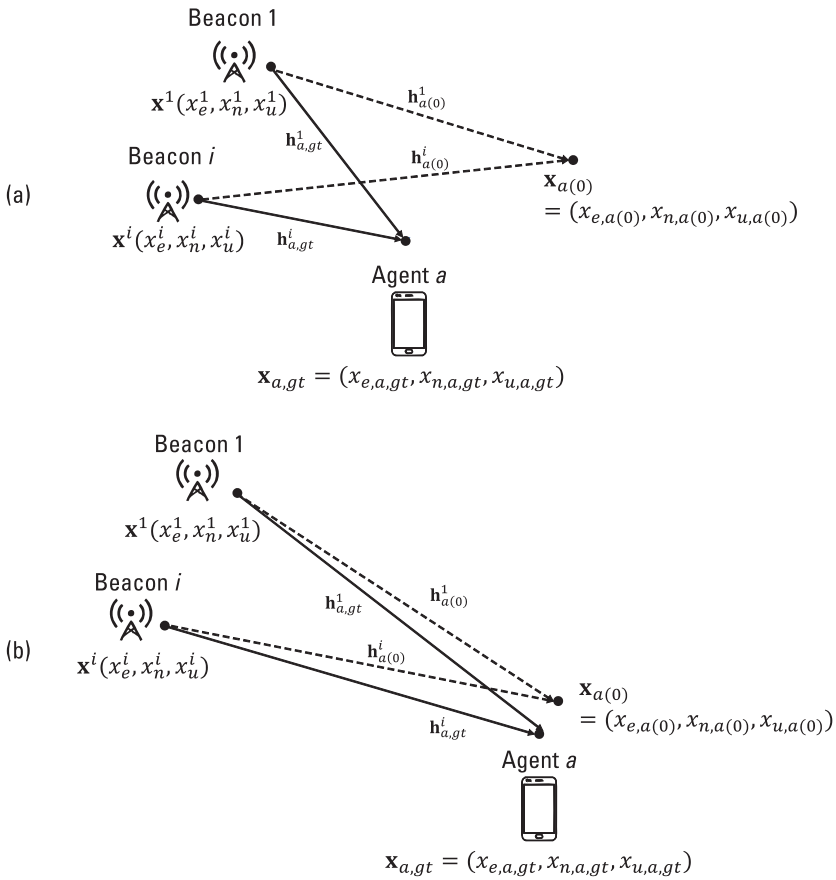

Figure 4.9 Illustrations of the accuracy of the initial guess used for the ILS method: (left) poor initial guess, and (right) accurate initial guess.

$$\begin{aligned} d_a^i(\mathbf{x}_a) &\approx d_a^i(\mathbf{x}_{a(0)}) + \frac{\partial d_a^i}{\partial x_{e,a}}\delta x_{e,a} + \frac{\partial d_a^i}{\partial x_{n,a}}\delta x_{n,a} + \frac{\partial d_a^i}{\partial x_{u,a}}\delta x_{u,a} \\ &\quad + \frac{\partial^2 d_a^i}{\partial x_{e,a}^2}\delta x_{e,a}^2 + \frac{\partial^2 d_a^i}{\partial x_{n,a}^2}\delta x_{n,a}^2 + \frac{\partial^2 d_a^i}{\partial x_{u,a}^2}\delta x_{u,a}^2 \\ &= d_a^i(\mathbf{x}_{a(0)}) + \mathbf{h}_{a(0)}^i(\mathbf{x}_a - \mathbf{x}_{a(0)}) + \mathbf{g}_{a(0)}^i(\mathbf{x}_a - \mathbf{x}_{a(0)})^2 \end{aligned} \tag{4.109}$$

where $\mathbf{g}_{a(0)}^i$ denotes the second-order term of the linearized measurement model. Then the ILS can be conducted by:

$$\begin{aligned} d_a^i\left(\mathbf{x}_a\right) - d_a^i\left(\mathbf{x}_{a(0)}\right) &= \mathbf{h}_{a(0)}^i\left(\mathbf{x}_a - \mathbf{x}_{a(0)}\right) + \mathbf{g}_{a(0)}^i\left(\mathbf{x}_a - \mathbf{x}_{a(0)}\right)^2 \\ \delta\mathbf{z}_a &= \mathbf{H}_{a(0)}\delta\mathbf{x}_a + \mathbf{G}_{a(0)}\delta\mathbf{x}_a^2 \end{aligned} \tag{4.110}$$

Another direction to handle the issue of a poor initial guess is to apply the robust estimation such as an M-estimator and coarse-to-fine approach that introduced in Chapter 2. By relaxing the nonconvexity (in the cost of a higher computational load in general) of the LS problem, the impact caused by the poor initial guess can be mitigated.

References

[1] Giovanelli, D., et al., "Bluetooth-Based Indoor Positioning Through ToF and RSSI Data Fusion," *2018 International Conference on Indoor Positioning and Indoor Navigation (IPIN)*, September 24–27, 2018, pp. 1–8.

[2] Hengyotmark, S., et al., "Pseudo-Ranging Based on Round-Trip Time of Bluetooth Low Energy Beacons," in *Recent Advances in Information and Communication Technology*, P. Meesad, S. Sodsee, and H. Unger, (eds.), New York: Springer International Publishing, 2018, pp. 202–211.

[3] Luo, H., et al., "Integration of GNSS and BLE Technology with Inertial Sensors for Real-Time Positioning in Urban Environments," *IEEE Access*, Vol. 9, 2021, pp. 15744–15763.

[4] Yu, N., et al., "A Precise Dead Reckoning Algorithm Based on Bluetooth and Multiple Sensors," *IEEE Internet of Things Journal*, Vol. 5, No. 1, 2018, pp. 336–351.

[5] Sheng, Z., and J. K. Pollard, "Position Measurement Using Bluetooth," *IEEE Transactions on Consumer Electronics*, Vol. 52, No. 2, 2006, pp. 555–558.

[6] Monfared, S., et al., "AoA-Based Iterative Positioning of IoT Sensors with Anchor Selection in NLOS Environments," *IEEE Transactions on Vehicular Technology*, Vol. 70, No. 6, 2021, pp. 6211–6216.

[7] Ye, F., et al., "A Low-Cost Single-Anchor Solution for Indoor Positioning Using BLE and Inertial Sensor Data," *IEEE Access*, Vol. 7, 2019, pp. 162439–162453.

[8] Gezici, S., et al., "Localization Via Ultra-Wideband Radios: A Look at Positioning Aspects for Future Sensor Networks," *IEEE Signal Processing Magazine*, Vol. 22, No. 4, 2005, pp. 70–84.

[9] Dardari, D., et al., "Ranging with Ultrawide Bandwidth Signals in Multipath Environments," *Proceedings of the IEEE*, Vol. 97, No. 2, 2009, pp. 404–426.

[10] Alavi, B., and K. Pahlavan, "Modeling of the TOA-Based Distance Measurement Error Using UWB Indoor Radio Measurements," *IEEE Communications Letters*, Vol. 10, No. 4, 2006, pp. 275–277.

[11] Alsindi, N. A., B. Alavi, and K. Pahlavan, "Measurement and Modeling of Ultrawideband TOA-Based Ranging in Indoor Multipath Environments," *IEEE Transactions on Vehicular Technology*, Vol. 58, No. 3, 2009, pp. 1046–1058.

[12] Taponecco, L., A. A. D. Amico, and U. Mengali, "Joint TOA and AOA Estimation for UWB Localization Applications," *IEEE Transactions on Wireless Communications*, Vol. 10, No. 7, 2011, pp. 2207–2217.

[13] Luo, Y., and C. L. Law, "Indoor Positioning Using UWB-IR Signals in the Presence of Dense Multipath with Path Overlapping," *IEEE Transactions on Wireless Communications*, Vol. 11, No. 10, 2012, pp. 3734–3743.

[14] Joon-Yong, L., and R. A. Scholtz, "Ranging in a Dense Multipath Environment Using an UWB Radio Link," *IEEE Journal on Selected Areas in Communications*, Vol. 20, No. 9, 2002, pp. 1677–1683.

[15] Adams, J. C., et al., "Ultra-Wideband for Navigation and Communications," *2001 IEEE Aerospace Conference Proceedings (Cat. No. 01TH8542)*, Vol. 2, March 10–17, 2001, pp. 2/785–2/792.

[16] Angelis, G. D., A. Moschitta, and P. Carbone, "Positioning Techniques in Indoor Environments Based on Stochastic Modeling of UWB Round-Trip-Time Measurements," *IEEE Transactions on Intelligent Transportation Systems*, Vol. 17, No. 8, 2016, pp. 2272–2281.

[17] Zhu, D., and K. Yi, "EKF Localization Based on TDOA/RSS in Underground Mines Using UWB Ranging," *2011 IEEE International Conference on Signal Processing, Communications and Computing (ICSPCC)*, September 14–16, 2011, pp. 1–4.

[18] Bocquet, M., C. Loyez, and A. Benlarbi-Delai, "Using Enhanced-TDOA Measurement for Indoor Positioning," *IEEE Microwave and Wireless Components Letters*, Vol. 15, No. 10, 2005, pp. 612–614.

[19] Bottigliero, S., et al., "A Low-Cost Indoor Real-Time Locating System Based on TDOA Estimation of UWB Pulse Sequences," *IEEE Transactions on Instrumentation and Measurement*, Vol. 70, 2021, pp. 1–11.

[20] Mahfouz, M. R., et al., "Investigation of High-Accuracy Indoor 3-D Positioning Using UWB Technology," *IEEE Transactions on Microwave Theory and Techniques*, Vol. 56, No. 6, 2008, pp. 1316–1330.

[21] Pierucci, L., and P. J. Roig, "UWB Localization on Indoor MIMO Channels," *2005 International Conference on Wireless Networks, Communications and Mobile Computing*, Vol. 2, June 13–16, 2005, pp. 890–894.

[22] Zhang, Y., et al., "High Resolution 3-D Angle of Arrival Determination for Indoor UWB Multipath Propagation," *IEEE Transactions on Wireless Communications*, Vol. 7, No. 8, 2008, pp. 3047–3055.

[23] Wen, F., and C. Liang, "Fine-Grained Indoor Localization Using Single Access Point with Multiple Antennas," *IEEE Sensors Journal*, Vol. 15, No. 3, 2015, pp. 1538–1544.

[24] Zhao, B., et al., "A Tensor-Based Joint AoA and ToF Estimation Method for Wi-Fi Systems," *IEEE Wireless Communications Letters*, Vol. 10, No. 11, 2021, pp. 2543–2546.

[25] Golden, S. A., and S. S. Bateman, "Sensor Measurements for Wi-Fi Location with Emphasis on Time-of-Arrival Ranging," *IEEE Transactions on Mobile Computing*, Vol. 6, No. 10, 2007, pp. 1185–1198.

[26] Ma, C., et al., "Wi-Fi RTT Ranging Performance Characterization and Positioning System Design," *IEEE Transactions on Mobile Computing*, Vol. 21, No. 2, 2022, pp. 740–756.

[27] Retscher, G., "Fundamental Concepts and Evolution of Wi-Fi User Localization: An Overview Based on Different Case Studies," *Sensors*, Vol. 20, No. 18, 2020, p. 5121, https://www.mdpi.com/1424-8220/20/18/5121.

[28] Diggelen, F. V., R. Want, and W. Wang, "How to Achieve 1-Meter Accuracy in Android," *GPS World*, July 3, 2018, https://www.gpsworld.com/how-to-achieve-1-meter-accuracy-in-android/.

[29] Kumarasiri, R., et al., "An Improved Hybrid RSS/TDOA Wireless Sensors Localization Technique Utilizing Wi-Fi Networks," *Mobile Networks and Applications*, Vol. 21, No. 2, 2016, pp. 286–295.

[30] Xie, T., et al., "A Wi-Fi-Based Wireless Indoor Position Sensing System with Multipath Interference Mitigation," *Sensors*, Vol. 19, No. 18, 2019, p. 3983, https://www.mdpi.com/1424-8220/19/18/3983.

[31] Dwivedi, S., et al., "Positioning in 5G Networks," *IEEE Communications Magazine*, Vol. 59, No. 11, 2021, pp. 38–44.

[32] Huang, J., J. Liang, and S. Luo, "Method and Analysis of TOA-Based Localization in 5G Ultra-Dense Networks with Randomly Distributed Nodes," *IEEE Access*, Vol. 7, 2019, pp. 174986–175002.

[33] Koivisto, M., et al., "Joint Device Positioning and Clock Synchronization in 5G Ultra-Dense Networks," *IEEE Transactions on Wireless Communications*, Vol. 16, No. 5, 2017, pp. 2866–2881.

[34] Peral-Rosado, J. A. D., et al., "Exploitation of 3D City Maps for Hybrid 5G RTT and GNSS Positioning Simulations," *ICASSP 2020—2020 IEEE International Conference on Acoustics, Speech and Signal Processing (ICASSP)*, May 4–8, 2020, pp. 9205–9209.

[35] Deng, Z., et al., "A TDOA and PDR Fusion Method for 5G Indoor Localization Based on Virtual Base Stations in Unknown Areas," *IEEE Access*, Vol. 8, 2020, pp. 225123–225133.

[36] Menta, E. Y., et al., "On the Performance of AoA–Based Localization in 5G Ultra–Dense Networks," *IEEE Access*, Vol. 7, 2019, pp. 33870–33880.

[37] "IEEE Standard for a Precision Clock Synchronization Protocol for Networked Measurement and Control Systems," *IEEE Std. 1588-2019 (Revision of IEEE Std 1588-2008)*, 2020, pp. 1–499.

{AU: Provide publication date}

{AU: Provide complete publication information}

[38] Lipinski, M., "The White Rabbit Project,", https://white-rabbit.web.cern.ch/.

[39] Mills, D., et al., "Network Time Protocol Version 4: Protocol and Algorithms Specification,", 2070-1721, 2010.

[40] GPS.gov, "GPS Standard Positioning Service (SPS) Performance Standard," 2020, https://www.gps.gov/technical/ps/.

[41] International Telecommunication Union, "G.8262.1: Timing Characteristics of Enhanced Synchronous Equipment Slave Clock," 2022, https://www.itu.int/rec/T-REC-G.8262.1-202211-I/en.

[42] Zhang, F., et al., "Ultrawideband-Based Real-Time Positioning with Cascaded Wireless Clock Synchronization Method," *IEEE Internet of Things Journal*, Vol. 11, No. 9, 2024, pp. 16731–16745.

[43] Blankenship, Y., and Z. Zou, "Paving the Way for a Wireless Time Sensitive Networking Future," Ericsson, 2023, https://www.ericsson.com/en/blog/2023/9/paving-the-way-for-wireless-time-sensitive-networking-future.

[44] Lindh, J., *Application Report: Bluetooth Lowenergy Beacons*, Texas Instruments, 2016.

[45] Petovello, M., "Clock Offsets in GNSS Receiver " *InsideGNSS*, 2011.

[46] Goldsmith, A., *Wireless Communications*, Cambridge, U.K.: Cambridge University Press, 2005.

[47] Zanella, A., "Best Practice in RSS Measurements and Ranging," *IEEE Communications Surveys & Tutorials*, Vol. 18, No. 4, 2016, pp. 2662–2686.

[48] Patwari, N., et al., "Relative Location Estimation in Wireless Sensor Networks," *IEEE Transactions on Signal Processing*, Vol. 51, No. 8, 2003, pp. 2137–2148.

[49] Cheung, K. W., et al., "Least Squares Algorithms for Time-of-Arrival-Based Mobile Location," *IEEE Transactions on Signal Processing*, Vol. 52, No. 4, 2004, pp. 1121–1130.

[50] Fang, B. T., "Simple Solutions for Hyperbolic and Related Position Fixes," *IEEE Transactions on Aerospace and Electronic Systems*, Vol. 26, No. 5, 1990, pp. 748–753.

[51] Chan, Y. T., and K. C. Ho, "A Simple and Efficient Estimator for Hyperbolic Location," *IEEE Transactions on Signal Processing*, Vol. 42, No. 8, 1994, pp. 1905–1915.

[52] Reza, R. I., *Data Fusion for Improved TOA/TDOA Position Determination in Wireless Systems*, Virginia Tech, 2000.

[53] Foy, W., "Position-Location Solutions by Taylor-Series Estimation," *IEEE Transactions on Aerospace and Electronic Systems*, Vol. AES-12, No. 2, 1976, pp. 187–194.

[54] Doğançay, K., "Bearings-Only Target Localization Using Total Least Squares," *Signal Processing*, Vol. 85, No. 9, 2005, pp. 1695–1710.

[55] Lingren, A. G., and K. F. Gong, "Position and Velocity Estimation Via Bearing Observations," *IEEE Transactions on Aerospace and Electronic Systems*, Vol. AES-14, No. 4, 1978, pp. 564–577.

[56] Doğançay, K., "On the Bias of Linear Least Squares Algorithms for Passive Target Localization," *Signal Processing*, Vol. 84, No. 3, 2004, pp. 475–486.

[57] Dogancay, K., and G. Ibal, "Instrumental Variable Estimator for 3D Bearings-Only Emitter Localization," *2005 International Conference on Intelligent Sensors, Sensor Networks and Information Processing*, December 5–8, 2005, pp. 63–68.

[58] Brown, R. G., and P. Y. C. Hwang, *Introduction to Random Signals and Applied Kalman Filtering*, Third Edition, New York: John Wiley & Sons, 1997.

[59] Feng, R., et al., "Wireless Channel Parameter Estimation Algorithms: Recent Advances and Future Challenges," *China Communications*, Vol. 15, No. 5, 2018, pp. 211–228.

[60] Zwirello, L., et al., "UWB Localization System for Indoor Applications: Concept, Realization and Analysis," *Journal of Electrical and Computer Engineering*, Vol. 2012, 2012, p. 849638.